DIPLOMARBEIT

Titel der Diplomarbeit

"QCD Analysis of Hadron Multiplicities and Determination of Fragmentation Functions in e^+e^--Annihilation from BELLE and LEP Data"

angestrebter akademischer Grad

Magister/Magistra der Naturwissenschaften

(Mag.rer.nat)

Verfasser:	Patricia M. Francisconi
Matrikelnummer:	0300798
Studienrichtung (lt. Studienblatt):	Physik
Betreuer:	Ao. Univ.-Prof. Dr. Walter Grimus

Wien, am 15. Dezember 2009

About this Document:

This document was created using free software.
For all pictures and plots from other sources used in this document, references are provided and it was attempted to obtain permission for their use from every author and creator. The author of this thesis asks for notification should any copyrights still be violated.
This document was compiled using LaTeX2e .

“Most people say that is it is the intellect which makes a great scientist. They are wrong: it is character. ”
Albert Einstein

Acknowledgements

First and foremost, my special thanks go to Prof. Matthias Grosse-Perdekamp for his tremendous help and support. His advising and encouragement was crucial to the outcome of this thesis.

I would also like to extend very special thanks to Ralf Seidl for his immensely helpful constructive criticism and advising during many BELLE meetings and the writing of this thesis.
Under the guidelines of those two excellent researchers and physicists, I was able to present scientific results.

Josh Rubin, who was always there to help with programming, debugging and understanding the darkest abyss of Mathematica syntax, deserves a very special thanks.

My deep appreciation also goes to Penny Siegler and Denise Donnoly, who were immensely helpful with everything regarding administration, bureaucracy and necessary paperwork at the University of Illinois.

Martin Leitgab, who has been very helpful in the process of settling in to the research group and often had a word of advice, deserves a heartfelt "Thank You", as well.

I would also like to thank Prof. Walter Grimus, who agreed to be my advisor in Vienna and accepted my research conducted at the University of Illinois. Without his blessing and support, all the effort would have been rendered useless.

Without the combined effort and help of those involved, this project would have never been possible.

Last but not least, I would like to thank my parents, who have been incredibly supportive and equipped me with all the tools necessary to complete this important stage in my life. Without their help I would not have had the chance to experience the joy of being a student at home as well as abroad.

Contents

Chapter 1

Introduction, Motivation and Outline

1.1 Introduction and Motivation

The understanding of hadron production is a fairly complex problem, that can only be solved by combining a theoretical framework with experimental results. The theory used to explain such hadronization processes is Quantum Chromodynamics, the gauge theory of strong interactions (see Chapter 2) [1].
Processes where we can observe a hadron in a final state can be described through perturbative cross sections and two non-perturbative, universal functions: parton distribution (PDF) and fragmentation functions (FF). PDFs are interpreted as probability distributions for finding a parton inside a hadron with a certain fraction of the hadron's momentum, whereas FFs describe probability distributions of finding a hadron, coming from a parton, with a certain fraction of the parton's momentum.
Essentially, one can say that PDFs describe an initial particle, whereas the dimensionless fragmentation functions describe a final-state, single-particle energy distribution in a hard scattering process.
The perturbative component can be calculated completely in Quantum Chromodynamics through perturbation theory, without additional input from experiments.
Perturbative QCD (pQCD) can only be used to describe scattering processes at very high energies, which has its roots in the asymptotic freedom of the theory, explained in more detail in Chapter 2. Therefore functions describing the low energy regions need to be extracted from data and have found to be sensitive to the details of an interaction to an extent that no

current model can match.
Once obtained they represent a fundamental tool for a more detailed look at the nucleon structure.
One big advantage of FFs is their independence of the process. They describe the properties of a parton and are therefore the same, regardless of the process by which it is produced.
Not only does this allow us to use the same function at different energy scales but also in entirely different experimental setups. So even though traditionally, most fragmentation function analyses were performed with data from e^+e^--experiments, the functions obtained are just as valid in a proton-proton-collision setup.
This leads to a multitude of different possible applications in data analysis, for instance at the Relativistic Heavy Ion Collider RHIC, at the Brookhaven National Laboratory in New York, for Semi-Inclusive Deep Inelastic Scattering experiments or for Proton-Proton collisions [2].
As a result of longterm, precise measurements, the knowledge on PDFs has reached a point where they provide accurate information on the proton structure [3]. The different experiments and analysis agree with each other within the small estimated uncertainties and are fully consistent with predictions coming from QCD [4].
Following the example of PDFs, fragmentation functions have been evolving quickly, unfortunately without yet reaching the same precision [5–8]. Especially the gluon fragmentation function has not yet been extracted with sufficient accuracy to be used in describing nucleon substructure and precise parton distributions within the desired error margins.
Detailed knowledge of quark and gluon fragmentation functions will give us an accurate insight into hadron structure and provide us with additional information concerning the proton spin [9].
The inclusive production of a single charged hadron $e^+e^- \to (\gamma, Z) \to hX$ has been measured at many different center-of-mass (c.m.) energies, where a large number of precise sets of data from various collaborations have become available, none the less it has so far been impossible to distinguish between quark and antiquark fragmentation from e^+e^--annihilation alone. Even the possibility of disentangling favored and disfavored fragmentation functions is limited and accurate predictions can only be made through the use of data from Semi Inclusive Deep Inelastic Scattering (SIDIS) experiments, where mostly up-quarks appear in the initial state.
Favored fragmentation functions denote functions from a quark or antiquark that is a constituent of the hadron in the quark model, whereas disfavored fragmentations come from the so-called sea quarks.

The ability to distinguish between individual quarks, or favored and disfavored fragmentation, is highly dependent on so-called "tagging" (which identifies the quark flavor that a jet comes from) and assumptions obtained from Monte-Carlo simulations [10].
Due to the lack of precise enough data at the significant energy scale (Z-Boson mass, where electroweak couplings become equal), the gluon fragmentation is not yet well enough constrained.
For the first time, the BELLE experiment (see Chapter 3), provides the possibility of precision measurements as it offers very high statistics combined with particle identification over a broad range of hadron momenta. The separate measurement of different hadrons, and their charges (pi^+, π^-, K^+, K^-) [28] opens a door to a more detailed extraction of fragmentation functions. The advantage of process independence in FFs as well as the opportunity to use the newest and most accurate data inspired the production of this thesis.
The aim is to extract fragmentation functions with high accuracy and little uncertainties [11].

1.2 Fragmentation Functions "Historically"

1.2.1 The Pioneers of Fragmentation Functions

[1] One can say that the pioneers of fragmentation function calculation are S. Albino [12], B. A. Kniehl, G. Kramer and B. Pötter [13, 14] whose research first dealt with the issue of extracting fragmentation functions up to Next-to-Leading Order from e^+e^--annihilation data.

1.2.2 The Kniehl-Kramer-Poetter Analysis (KKP)

[2] B.A.Kniehl, G.Kramer, B.Pötter's analysis, similarly to the one performed by S. Kumano, determined fragmentation functions for charged Pions, Kaons and protons by fitting to e^+e^--annihilation data.
The data sets used include DELPHI [15], SLD [16] with quark flavor separation and data sets from ALEPH [17], DELPHI, SLD and TPC without flavor separation.
DELPHI and ALEPH are experiments performed at the Large-Electron-Positron Collider at CERN in Switzerland, the SLD data comes from a collaboration working on electron-positron annihilation at the Stanford Linear Accelerator Center (SLAC) and the TPC detector is situated at CERN.
The c.m. energies used in the experiments are 29.0 and 91.2 GeV with the same key observable as in other FF analyses: a scaled-momentum distribution normalized to the hadronic cross section (see Chapter 2).
The parametrization characterizing the z-dependence of the fragmentation functions used by KKP was a fairly simple one.
The Ansatz $D_q^H = Nz^\alpha(1-z)^\beta$, only using 3 parameters, has proven to be a fairly accurate initial distribution, with the high z-regions being accounted for through the z^α-term and the low z-regions through $(1-z)^\beta$.
After Evolution with Q^2, performed in Mellin space (see Chapter 2), the function was fitted to the data sets producing fairly accurate results: see Fig. 1.1

In the analysis performed by M.Hirai, S. Kumano, T.-H. Nagai and K. Sudoh (HKNS) [8, 18, 19] a similar parametrization as in KKP [13] was used. HKNS, along with DSS were the first ones to incorporate a detailed look at errors and uncertainties.

[1]Details and Notation as well as Abbreviations used in this Chapter are explained more thoroughly in Chapter 2.

[2]according to Ref. [13] with notation from [5], unless otherwise stated

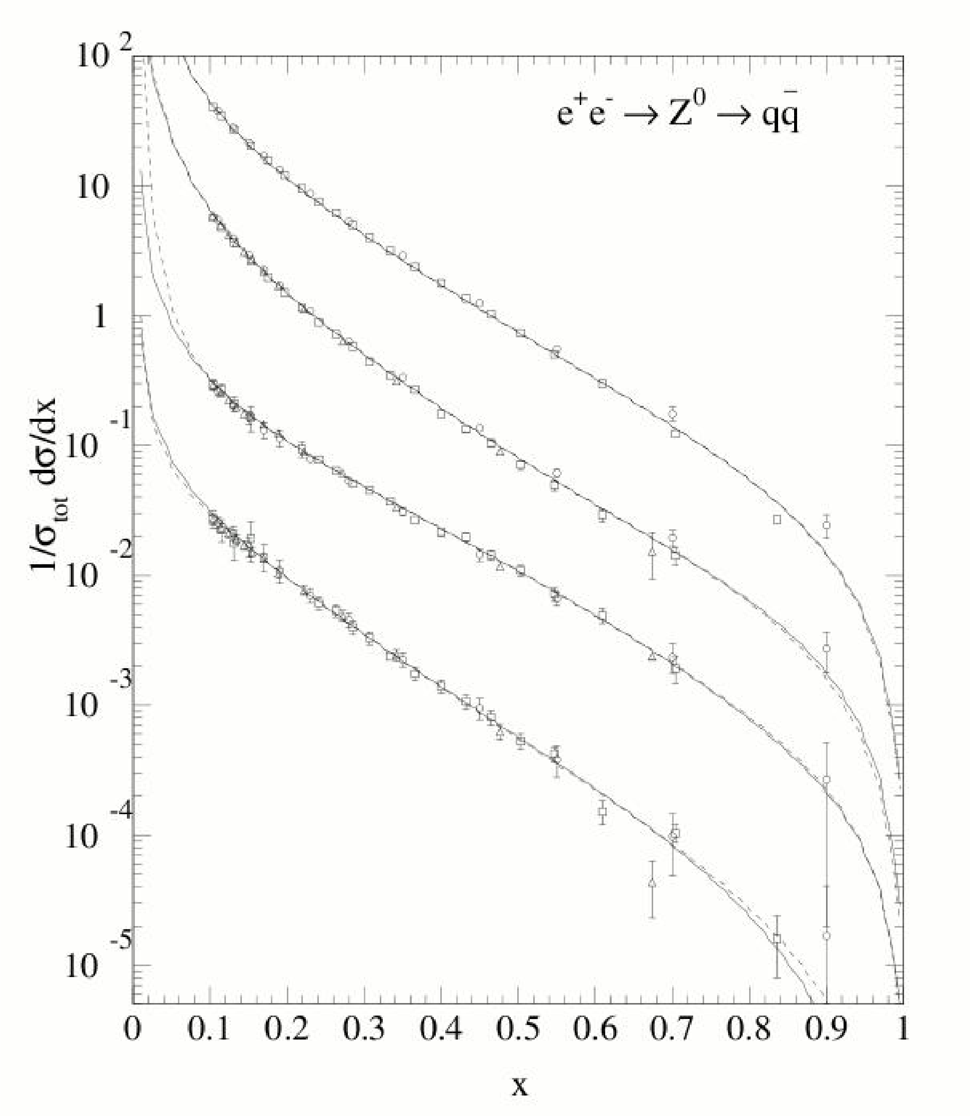

Figure 1.1: Normalized cross section at c.m.s energy of 91.2 GeV, with Leading Order lines dashed and Next-To-Leading-Order lines solid, data from ALEPH (represented by triangles), DELPHI (circles), SLD (squares) [13, 14].

1.2.3 The DeFlorian-Stratmann-Sassot Analysis (DSS)

A newer and more advanced analysis has been performed by M. Stratmann, D. de Florian and R. Sassot [5].
The main difference between theirs and previous analyses is the initial parametrization for z and the data used for fitting, as well as the fact that it includes a large number of different experimental setups.
The data used by DSS does not only include e^+e^--data but also data from semi inclusive deep inelastic scattering (SIDIS) experiments and hadron-hadron collisions.
The big advantage of using SIDIS data lies in their sensitivity to individual quark and antiquark flavors, which is not accessible through e^+e^-.
Hadron-hadron collisions are extremely sensitive to gluon fragmentation due to the dominance of $gg \to gX$ for hadrons produced at low to medium transverse momenta, as well as to fragmentation functions at very high z.
The cross sections for SIDIS and proton-proton-collisions are omitted here since the focus of this analysis lies on e^+e^--data and can be found in Ref. [5, 11]. Another difference between this analysis and previous ones is a more complicated but therefore also more flexible parametrization:

$$D_i^H(z, \mu_0) = \frac{N_i z^{\alpha_i}(1-z)^{\beta_i}[1+\gamma_i(1-z)^{\delta_i}]}{B[2+\alpha_i, \beta_i+1] + \gamma_i B[2+\alpha_i, \beta_i+\delta_i+1]} \tag{1.1}$$

with B[...] being the Euler-Beta function, resulting from the normalization of the parametrization.
This initial distribution for the fragmentation function has proven to be more accurate, due to the higher number of free parameters $(n, \alpha, \beta, \gamma, \delta)$ and the additional information from SIDIS and proton-proton data (see Fig. 1.2).

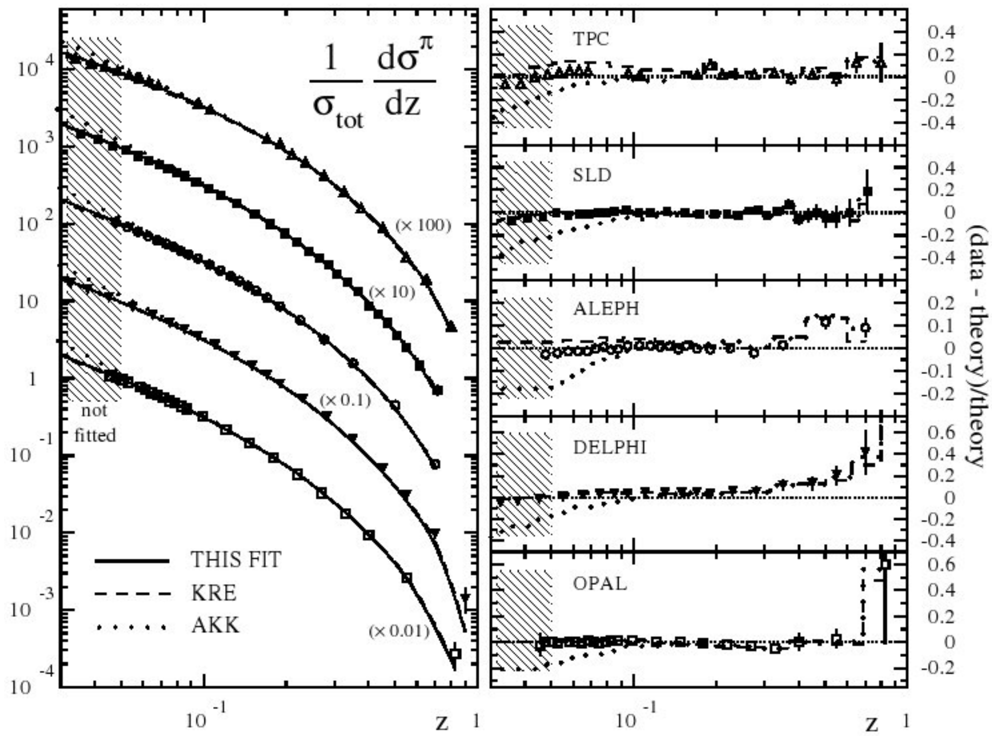

Figure 1.2: comparing the results of the NLO fit to the data sets, dotted lines: results with previous parametrizations [5].

1.3 Outline

In this thesis, a QCD analysis of BELLE and LEP data (see Chapter 3), as well as an evolution with Q^2 in Mellin space was performed and fragmentation functions were calculated. This allows us to compare fragmentation functions at different energies, through which the precision of fragmentation function calculation is raised significantly.
Chapter 2 will focus on the theoretical framework of the analysis and explain fragmentation in QCD, as well as look into all properties needed to conduct such an analysis. This should help give an understanding of how hadrons are produced and the way by which the concept of asymptotic freedom influences the process.
In Chapter 3 an overview of the experiments used is given and their advantages are explained. The new availability of the BELLE data has inspired the analysis presented in this thesis with the goal of extracting fragmentation functions with high accuracy. This is the first analysis containing data from BELLE, where lower energies are taken into account that have been omitted by previous experiments, due to the fact that other detectors weren't sensitive enough in those regions (see Chapter 3).
Chapter 4 will contain details regarding the fitting method, the actual calculations of the relevant DGLAP evolution equations and the properties needed for it. Used symmetry relations and their reasoning can be found in Chapter 4 as well. The complexity of the problem should become clear and possible difficulties encountered in the Q^2 evolution, along with a method for solving them will be explained.
The last chapter contains fit results with the parameters determined by the fit and possible discrepancies with the experimental data will be looked at. Details to functions and calculations, as well as the working code for this analysis can be found in the Appendix.

Chapter 2

QCD Framework

Due to the process-independence of fragmentation functions they are used in a large number of different experimental setups: e^+e^--annihilation, Proton-Proton-collisions, $e-\mu-\nu$-scattering off a proton or a nucleus as well as heavy ion collisions.
To open up the possibility of even finding any kind of physics beyond the Standard Model a detailed knowledge of Quantum Chromodynamics is necessary to predict cross sections of interactions.
Calculations in perturbative QCD have been found to give fairly accurate descriptions of cross sections up to Next-to-Leading Order (NLO) for a lot of different reactions and even up to Next-to-Next-to-Leading Order (NNLO) for some. The next step to a complete comprehension of QCD is the understanding of the non-perturbative parts [8].
The partons produced in hard scattering reactions, fragment into colorless, hadronic bound states.
Using the factorization theorem one can decompose the cross section of such processes into convolutions of perturbatively calculated hard scattering cross sections and two non perturbative, universal components: parton distribution functions, describing the partonic structure of the hadron and fragmentation functions, which deal with the details of the hadronization process. The precise knowledge of these three components is crucial to the description of hard scattering in pQCD and its continued success.
Without additional information other than the running coupling constant α_S (see Chapter 2.2), the hard scattering cross section (Eq. (2.2)) can be determined by calculating it purely perturbatively.
The actual transition of partons into hadrons takes place at a low energy scale of the order of 1 GeV and can not be calculated in pQCD. This non-perturbative component of hadronization can instead be described by Fragmentation Functions [1, 2, 5].

2.1 Fragmentation

For the purpose of looking at the hadron production only fragmentation functions $D_i^H(z, Q^2)$ are of interest and PDFs will be disregarded from here on out.
They can be interpreted as the probability distribution that a parton, produced at a short distance $\frac{1}{Q}$, fragments into a hadron, carrying a fraction z of the parent momentum k.[3]

2.1.1 e^+e^--annihilation:

The cross sections for SIDIS and hadron-hadron collisions are given in Chapter 1.3.3 and can be found in detail in Ref.[5].
Since only e^+e^--annihilation data is used in this analysis, the focus will be on the details of only that reaction.
The inclusive production of a single charged hadron in the annihilation process $e^+e^- \to (\gamma, Z \to hX)$ has been measured at a wide variety of different energies, which made it possible to determine quark and gluon fragmentation functions into hadrons.
The first part of the process is the creation of a quark-antiquark pair $e^+e^- \to q\bar{q}$ in Leading Order (LO), with a gluon in NLO $e^+e^- \to q\bar{q}g$, the second part is the production of a hadron from those partons, the fragmentation [8].
The cross section at c.m.s energy of $e^+e^- \to (\gamma, Z) \to hX$

$$\frac{1}{\sigma_{tot}} \frac{d\sigma^h}{dz} = \mathcal{F}^H(z, Q^2) = \frac{\sigma_0}{\sum_q \hat{e}_q^2} \left[2F_1^H(z, Q^2) + F_L^H(z, Q^2)\right] \tag{2.1}$$

with $\mathcal{F}^H(z, Q^2)$ being the total fragmentation function.
Q^2 is the energy of the of the virtual γ- or Z-momentum squared in $e^+e^- \to \gamma, Z$ (with $Q^2 = s$, where $\frac{\sqrt{s}}{2}$ is beam energy). The hadron energy E_H is scaled to the beam energy $\frac{Q}{2} = \frac{\sqrt{s}}{2}$ and is denoted as $z = \frac{2p_H q}{Q^2} = \frac{2E_H}{\sqrt{s}}$, with p being the 3-momentum of the observed hadron in center-of-mass frame [5].

[3] Equations according to Ref. [20] with notation from [5], unless otherwise stated

The total hard scattering cross section, including NLO corrections of α_S and $\sigma_0 = \frac{4\pi\alpha_S^2(Q^2)}{Q^2}$ comes from $e^+e^- \to \gamma \to q\bar{q}(g)$ and $e^+e^- \to Z \to q\bar{q}(g)$ and is defined as

$$\sigma_{tot} = \sum_q \hat{e}_q^2 \sigma_0 [1 + \frac{\alpha_S(Q^2)}{\pi}] \tag{2.2}$$

where $\hat{e}_q^2$ are the electroweak charges (including the mass and decay width of the Z-Boson as well as the fractional electromagnetic quark charge) corresponding to the quark flavors q, which can be found in Appendix A of Ref. [21].
The fragmentation process comes from quarks, antiquarks and gluons, is represented by the sum of their contribution, so the total fragmentation function can be represented as a convolution of parton fragmentation functions $D_i^H(z, Q^2)$ and coefficient functions $C_i(z, Q^2)$ (App.A Ref. [21]), summed over all partons.
Coefficient functions are probabilities of creating a parton i with a certain fraction of the beam energy.
They can be expressed as a power series in α_S.
At lowest order α_S the coefficient functions for gluons are zero (as gluons only start appearing through a quark loop) while for quarks they are given by: $C_i(z, Q^2) = g_i\delta(1 - z)$ with g_i being the appropriate Yukawa coupling.

$$\begin{aligned}\mathcal{F}^H(z,Q^2) &= \sum_i C_i(z,Q^2) \otimes D_i^H(z,Q^2) \\ &= \sum_{i=\text{partons}} \int_z^1 \frac{d\zeta}{\zeta} C_i(\zeta,Q^2) D_i^H(\frac{z}{\zeta},Q^2)\end{aligned} \tag{2.3}$$

$$\begin{aligned}2F_1^H(z,Q^2) &= \sum_q \hat{e}^2 \left\{ \left[D_q^H(z,Q^2) + D_{\bar{q}}^H(z,Q^2) \right] + \right. \\ & \left. + \frac{\alpha_S(Q^2)}{2\pi} \left[C_q^1 \otimes (D_q^H + D_{\bar{q}}^H) + C_g^1 \otimes D_g^H \right] (z,Q^2) \right\}\end{aligned} \tag{2.4}$$

$$F_L^H(z,Q^2) = \frac{\alpha_S(Q^2)}{2\pi} \sum_q \hat{e}^2 \left[C_q^L \otimes (D_q^H) + D_{\bar{q}}^H) + C_g^1 \otimes D_g^H \right] (z,Q^2) \tag{2.5}$$

where "$\otimes$" denotes a convolution as written in Eq. (2.3).
The total fragmentation function is composed of transverse and longitudinal fragmentation.
The total energy distribution in energy fraction z and the polar angle Θ relative to the lepton axis, has a transverse and a longitudinal component. F_1 and F_L represent contributions from virtual bosons polarized accordingly and integrated over all angles the total fragmentation function become the sum of the transverse and longitudinal fragmentation functions the way stated above.
The average multiplicity of hadrons is defined through

$$n_H = \int_0^1 dz \mathcal{F}^H(z,Q^2). \tag{2.6}$$

Momentum conservation of the fragmenting parton in the hadronization process is simply given by

$$\sum_H \int_0^1 dzzD_i^H(z,Q^2) = 1 \tag{2.7}$$

which states that each parton will fragment into some hadron with 100% probability.

2.2 DGLAP Evolution

Perturbative QCD predicts an evolution of fragmentation and structure functions with the energy Q^2, rather than making predictions for the shape of the function itself. The actual function itself needs to be determined by fitting a sufficiently flexible parametrization to sets of data (see Chapter 1.3).
Once a fragmentation function is obtained for one set of data we are able to use the same function for different a energy input and experimental setup. Its evolution with increasing energy scale is governed by the so-called DGLAP evolution equations, which enable us to let one function run through multiple sets of data at different energies, first performed by Dokshitzer, Gribov, Lipatov, Altarelli and Parisi [22–24].
After the fit, the different fragmentation functions, for different partons, at different orders can then be distinguished through the coefficients in the parametrization used.[4]

DGLAP evolution equation:

$$\frac{\partial}{\partial \ln Q} D_i^H(z, Q^2) = \sum_j \int_z^1 \frac{dx}{x} \frac{\alpha_S}{2\pi} P_{ji}(x, \alpha_S) D_j^H(\frac{z}{x}, Q^2) \tag{2.8}$$

The splitting functions are P_{ji} as oppose to P_{ij} since the function D_j^H represents the fragmentation of the final parton. The P_{ji}s represent the probability for finding a parton i coming from a parton j with a certain fraction of the parent momentum. An example for one so-called splitting could be a quark, coming from the e^+e^- reaction radiating a gluon, that carries a certain energy of the quark momentum (see Fig. 2.1).

[4]Equations according to Ref.[20][6] with notation from [5], unless otherwise stated

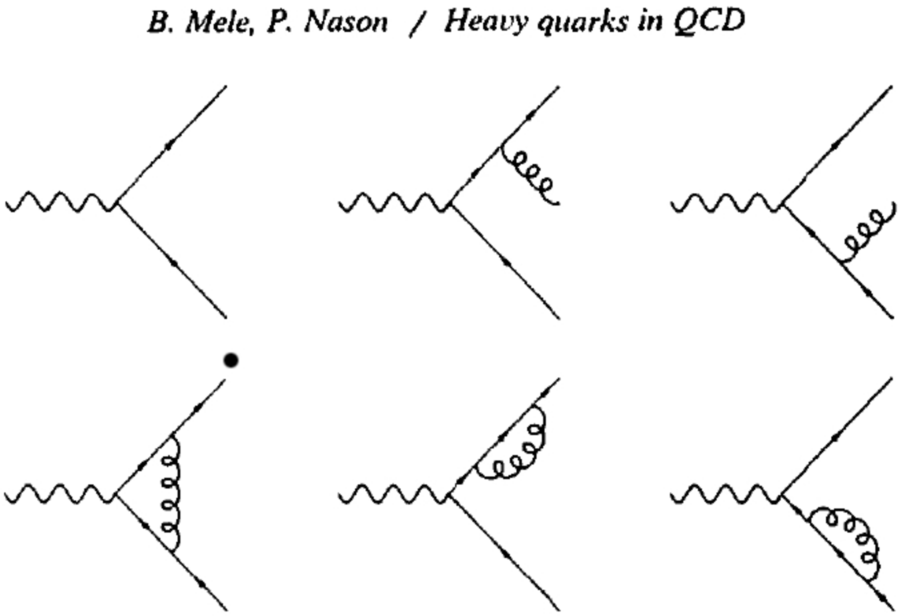

Figure 2.1: possible contributions to fragmentation functions [25]

The splitting functions have perturbative expansions:

$$P_{ji}(x, \alpha_S) = P_{ji}^{(0)}(x) + \frac{\alpha_S}{2\pi} P_{ji}^{(1)}(x) + ... \tag{2.9}$$

with the lowest order splitting functions $P_{ji}^{(0)}$ being the same for e^+e^- and DIS.
The outcome of the evolution is the same in both cases: with the increase of Q^2 one can observe a shifting of the z-distribution towards lower values (see Fig. 2.2) [20, 26, 27].

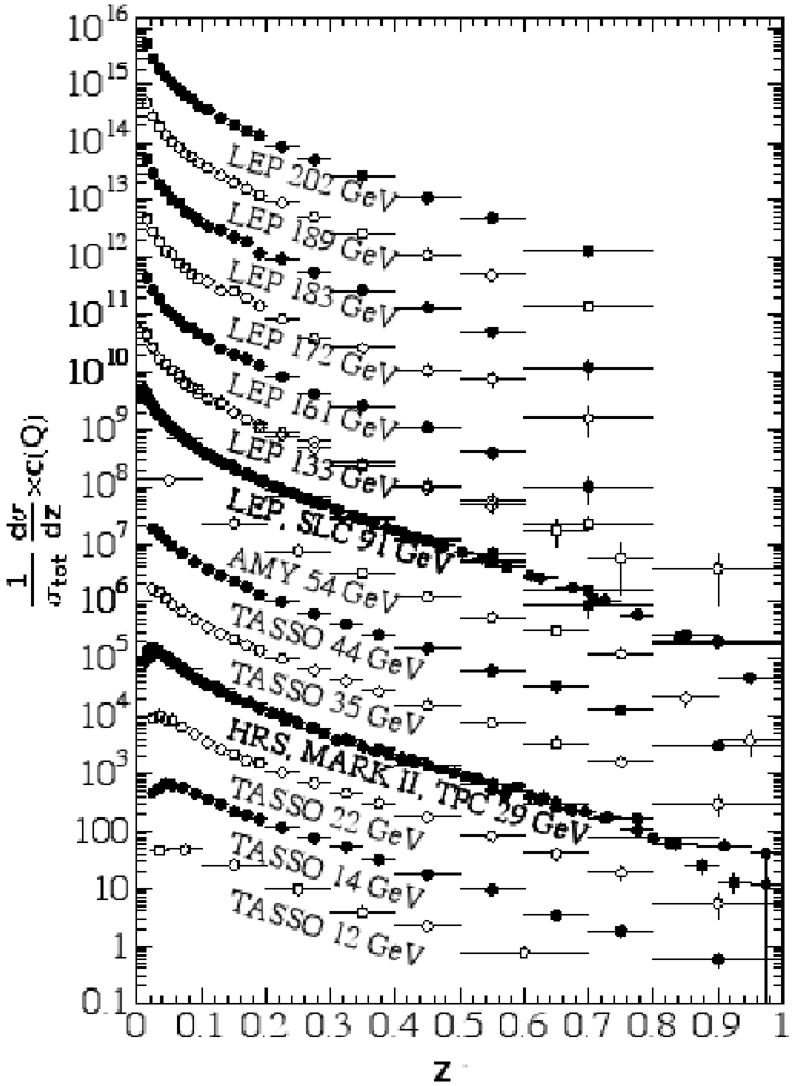

Figure 2.2: Fragmentation function from e^+e^- for all charged particles at different c.m. energies Q versus z, with Q going from 12 GeV to 189 GeV. This plot has been adapted from [20].

2.3 Mellin Technique

The actual calculation of fragmentation functions, including an evolution with Q^2 is a problem that includes a multitude of numerical convolution integrals, which leads to computational difficulties, due to the fact that those integrals need to be evaluated numerous times within the fit. To avoid this problem, like in the case of PDFs, the most common approach for solving the DGLAP equations is to take the Mellin moments of $D_j^H(x, Q^2)$ and $P_{ji}(z)$ with respect to z. To obtain those a Mellin transformation, that can be compared to a Fourier transformation, has to be performed.

$$D_{jM}^H(n, Q^2) = \int_0^1 dz z^{n-1} D_j^H(z, Q^2) \tag{2.10}$$

and P_{ji} respectively.
The advantage of working in Mellin space is the fact that the very time consuming numerical convolutions in z-pace of (2.3) and (2.8) turn into simple products in Mellin-space, which can be solved analytically for LO. In NLO they still have to be computed numerically but turn out to be much simpler expressions [28].
In the end the inverse Mellin transform remains the only numerical integral necessary.
One can now precalculate the Mellin moments of the needed properties $F_L^H(z, Q^2)$ and $F_1^H(z, Q^2)$ (see Eq. (2.4) and (2.5)). Finally the inverse Mellin transform links the obtained moments to the cross section and a fit can be performed.

$$D_j^H(z, Q^2) = \frac{1}{2\pi i} \int_C dn z^{-n} D_{jM}^H(n, Q^2) \tag{2.11}$$

where C is the contour in the complex n-plane, parallel to the imaginary axis and to the right of all singularities.
The exact contour used in this thesis, as well as parametrization, splitting- and coefficient functions in Mellin space can be found in Chapter 4 [29, 30].

2.4 Asymptotic Freedom and Running Coupling Constant

To be able to make detailed predictions within a theory it is necessary to look at the changes in the underlying force laws of that theory, with an energy scale. A useful mathematical structure to do so is the Renormalization Group, together with scale-invariance (see Appendix).
By varying the energy scale one can investigate the system with slightly different parameters, describing the interactions of the components of said system, as a coupling constant does.
The scale dependence of a coupling parameter of a theory is given by the Beta-Function.

$$2\beta\left(\alpha_S\right) = \mu\frac{\partial\alpha_S}{\partial\mu} = -\frac{\beta_0}{2\pi}\alpha_S^2 - \frac{\beta_1}{4\pi^2}\alpha_S^3 - \frac{\beta_2}{64\pi^3}\alpha_S^4 \tag{2.12}$$

where μ is the energy scale.
15

$$\beta_0 = 11 - \frac{2f}{3} \tag{2.13}$$

$$\beta_1 = 51 - \frac{19f}{3} \tag{2.14}$$

$$\beta_2 = 2857 - \frac{5033f}{9} + \frac{325f^2}{27} \tag{2.15}$$

Gauge theories with a non-abelian gauge field have the possibility of rendering the beta-function negative, which leads to an decrease of the coupling of the force with high energies (or momentum).
This is the principle of asymptotic freedom and has the consequence that

[5]Equations according to Ref. [20] with notation from [5], unless otherwise stated

perturbation theory can only be used for small coupling (or high energies). The scale dependence of the QCD or running coupling is governed by the β-function above and called the QCD renormalization group equation.

$$\mu \frac{d\alpha_S\left(\mu^2\right)}{d\mu^2} = -\frac{\beta_0}{2\pi}\alpha_S^2 - \frac{\beta_1}{4\pi^2}\alpha_S^3 - \frac{\beta_2}{64\pi^3}\alpha_S^4 - ... \tag{2.16}$$

for higher order, with f being the number of quarks with mass less than the energy scale μ. For LO β_1 and β_2 are 0.
The differential equation for α_S needs to be solved numerically. In order to do so, a constant of integration, as well as a dimensional parameter Λ, need to be introduced. A useful choice for the constant is the value for $\alpha_S(\mu_0)$. The dimensional parameter Λ provides a μ-dependence of α_S and its definition is arbitrary.
One way of defining Λ is to write the solution of the renormalization group equation as an expansion in inverse powers of $\ln(\mu^2)$

$$\begin{aligned}\alpha_S\left(\mu\right) \quad = \quad & \frac{4\pi}{\beta_0 \ln\left(\mu^2/\Lambda^2\right)} \cdot \left[1 - \frac{2\beta_1}{\beta_0^2}\frac{\ln\left[\ln\left(\frac{\mu^2}{\Lambda^2}\right)\right]}{\ln\left(\frac{\mu^2}{\Lambda^2}\right)} + \right.\\ & \left.\frac{4\beta_1^2}{\beta_0^4 \ln^2\left(\frac{\mu^2}{\Lambda^2}\right)}\left(\left(\ln\left[\ln\left(\frac{\mu^2}{\Lambda^2}\right)\right] - \frac{1}{2}\right)^2 + \frac{\beta_2\beta_0}{8\beta_1^2} - \frac{5}{4}\right)\right]\end{aligned} \tag{2.17}$$

This expression shows that QCD becomes strongly coupled at $\mu \sim \Lambda$ and illustrates the asymptotic freedom of $\alpha_S \rightarrow 0$ for $\mu \rightarrow \infty$.
Now all the properties needed for a QCD analysis are available [20, 31–33].

Chapter 3

Data Selection

3.1 Experiments and Data

The data included in this analysis was taken from two different e^+e^--annihilation experiments, of which an overview will be given in this chapter. Different hadrons at different energies are taken into account, which are related through DGLAP evolution.

From each experiment a separate data set for charge averaged (e.g. $\frac{K^+ + K^-}{2}$) Pions and one for Kaons was used.

3.1.1 BELLE

The data used from the BELLE experiment was obtained during the work on his Master's Thesis by Martin Leitgab, where the z-dependence of charge-resolved Pion and Kaon multiplicities at a center-of-mass energy of $\sqrt{s} = 10.52$ GeV, was measured [10]. The experiment is situated at the KEK-B accelerator in Japan and its advantage lies in the tracking and particle identification capabilities of the BELLE detector, as well as the large event sample available.

The KEK-B accelerator was constructed as a so-called B-factory at KEK in Japan, with the American counterpart being BARBAR/PEPII at SLAC in Stanford, USA, to investigate the B-meson-system and gain more insight in CP-violation. Both experiments use electron-positron annihilation.

The KEK-B accelerator creates high luminosity particle beams, which are observed with the BELLE detector, situated at an interaction point within KEK-B (see Fig. 3.1).

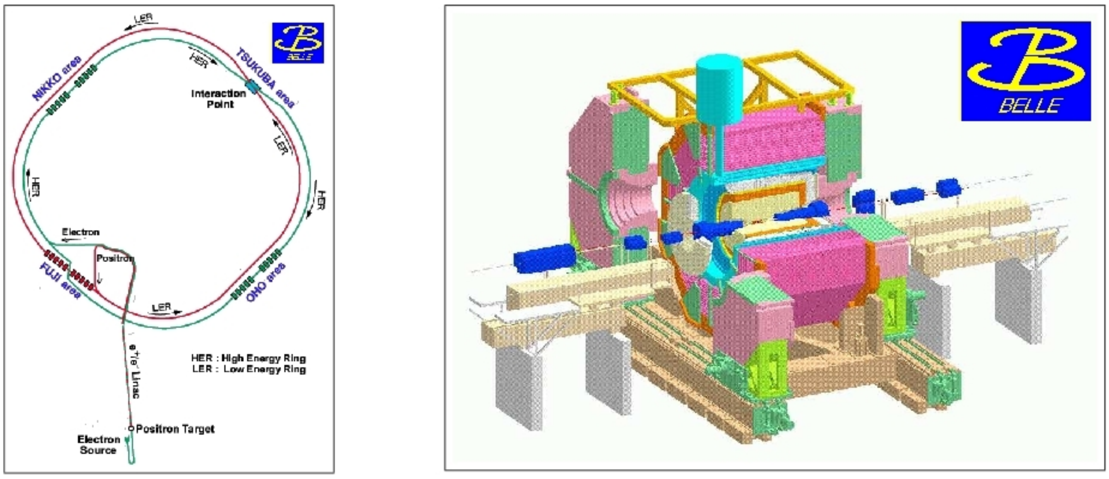

(a) (b)

Figure 3.1: KEK-B accelerator at Tsukuba, Japan (a) and BELLE detector at Tsukuba interaction area (b) [10].

The BELLE experiment measures rare B-decay modes and studies CP-violation and is operated at a center-of-mass energy at the $\Upsilon(4S)$ resonance at 10.58Gev/c^2. To be able to take background contributions into account the KEK-B accelerator is also operated at a lower cms energy of 10.52 GeV, where quark-antiquark contributions from flavors $\{u, d, s, c\}$ are produced. The BELLE detector is operational since 1999 and found evidence for CP-violation in 2001. The great detector performance allows its use in B-meson unrelated analyses as well, with a high level of precision.
For a visualization of the data see Fig. 3.2 and for a more detailed description of the detector see Ref. [10].

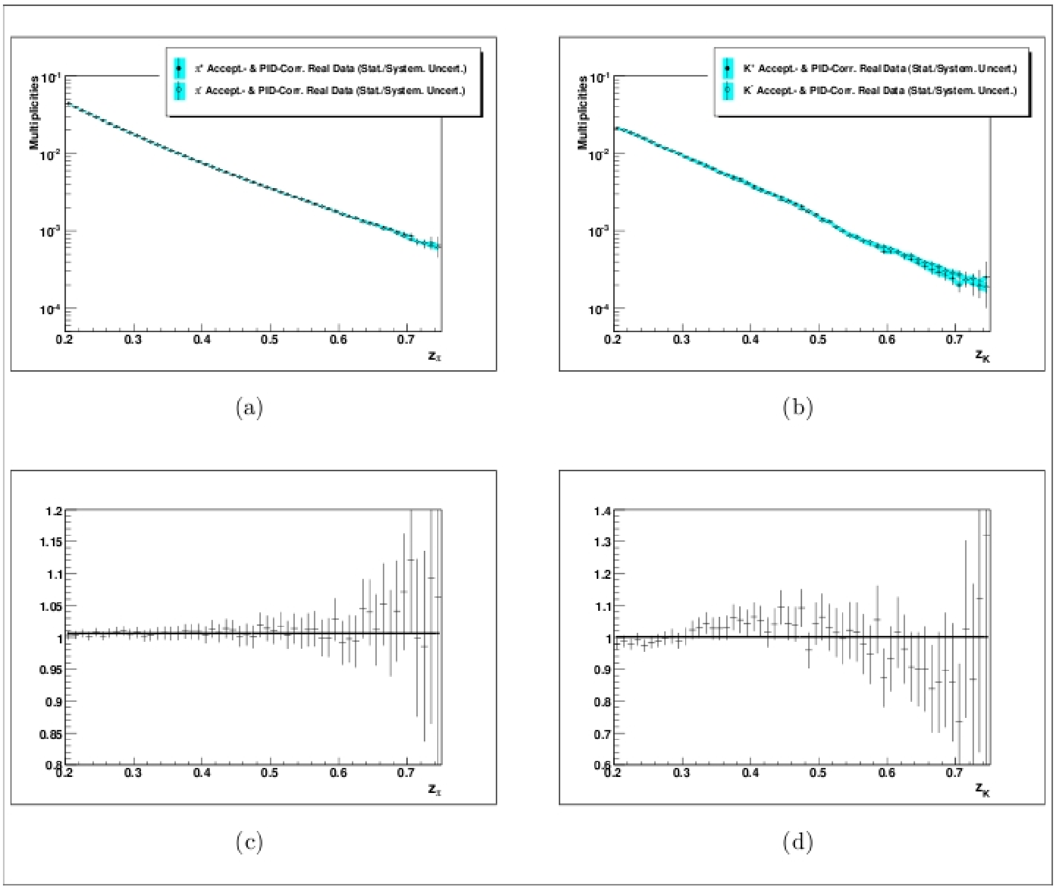

Figure 3.2: Acceptance- and PID-corrected multiplicities for species π^+ and π^- (a) and K^+ and K^- (b) from data sets of $\sim$ 7.6fb-1. Plots (c) and (d) show the ratios $\frac{\pi^+}{\pi^-}$ and $\frac{K^+}{K^-}$. Statistical uncertainties are propagated through the ratios in (c) and (d) [10].

3.1.2 OPAL

The data used in this analysis was obtained by G. Abbiendi et al., members of the OPAL collaboration, at center-of-mass energy near the Z^0 peak of about 91.5 GeV/c^2.
The OPAL (Omni-Purpose Apparatus for LEP) detector (see Fig. 3.3) was one of four detectors within the Large Electron-Positron (LEP) Collider at CERN, in Geneva, Switzerland, dismantled in 2001 to make way for the Large Hadron Collider (LHC).
In Ref. [34], used as reference for this analysis, the multiplicities for π^0, η, K^0 and charged particles in quark- and gluon jets, in 3-jet events were compared.
It was found that the ratio of particle multiplicities in gluon jets to those in quark jets, as a function of the jet-energy, for π^0, η, K^0, was independent of particle species, in accordance with QCD predictions [34].

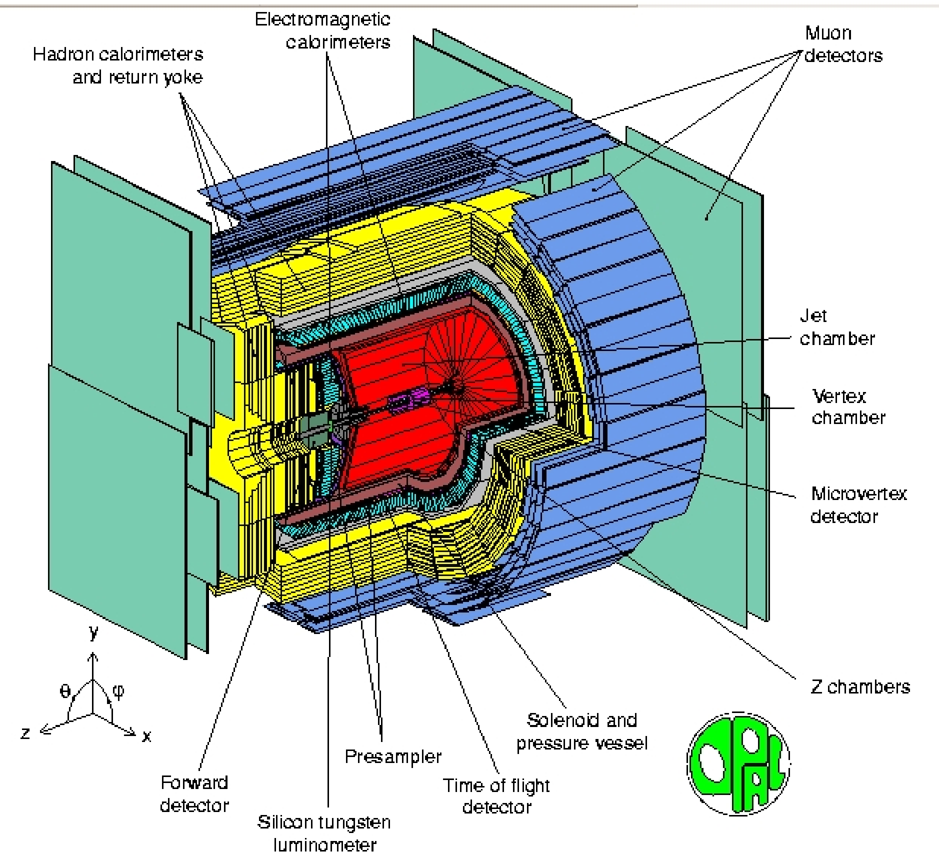

Figure 3.3: OPAL Detector at LEP experiment at CERN, Switzerland [35].

The ratio of the slope of the average particle multiplicity in gluon to that in quark jets was calculated and reached a precision of one standard deviation above the perturbative prediction.
For a visualization of the data see Fig. 3.4 and for a more detailed description of the experiment see Refs. [34, 35].

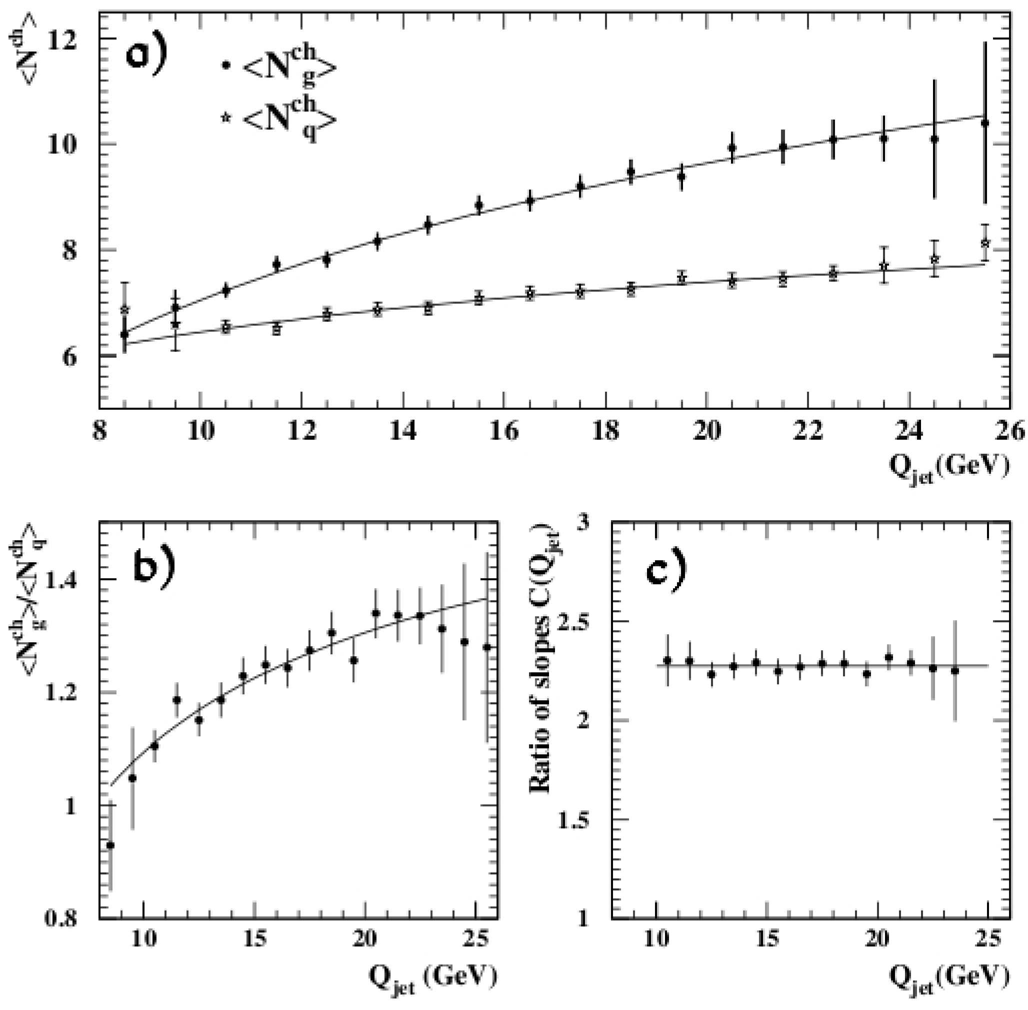

Figure 3.4: (a) average number of particles for pure quark- and gluon jets, with respect to Q_{jet}, including systematic errors (b) ratio of average charged particle multiplicities (c) same as (b), line is fit to a constant [34]

Chapter 4

Fit and Calculations

4.1 Parametrization and Symmetry Assumptions

The parameterizations at an initial energy scale μ_0, used in previous analyses, which were based only on e^+e^--annihilation data, were of a fairly simple functional form:

$$D_i^H = N_i z^{\alpha_i}(1-z)^{\beta_i} \tag{4.1}$$

A big limitation in the determination of fragmentation functions from only Single Inclusive Annihilation data is the fact that one can not distinguish between favored and disfavored fragmentation without previous assumptions. Only $D_{q+\bar{q}}^{H^+ + H^-}$ can be obtained from fitting SIA data sets. A distinction between quark and antiquark is only possible through including data from SIDIS experiments into the fit [5].
In the analysis performed by DSS [5] (Chapter 1.3.3) datasets from SIA, SIDIS and Hadron-Hadron collisions were used, which called for a more flexible parametrization, in order to account for all the information gotten from multiple experiments:

$$D_i^H(z,Q^2) = \frac{N_i z^{\alpha i}(1-z)^{\beta_i}\left[1+\gamma_i(1-z)^{\delta_i}\right]}{B\left[2+\alpha_i,\beta_i+1\right]+\gamma_i B\left[2+\alpha_i,\beta_i+\delta_i+1\right]} \tag{4.2}$$

, which will also be used in this analysis.
The Euler-Beta functions $B\,[...]$ and N_i have their origin in the normalization of D_i^H (see Eq. (2.7)). According to Ref. [5] setting $\delta_i = 0$ would introduce artificial connections in the behavior at different z regions and complicate the calculations of uncertainties.
Through comparison of previous analyses to the one performed by DSS one can see that the quality of the fit can be improved by the $(1-z)^{\delta_i}$ -term, due to the fact that small z regions have only a small effect on the calculation of fragmentation functions.
In this analysis as well as most previous ones, the initial energy scale μ_0 is set to 1 GeV, since the DGLAP evolution can only be performed from lower to higher energies and a sufficiently small μ_0 gives more flexibility towards using different experiments at various Q^2.
To reduce the computing time in the fit one can assume certain symmetries that will not greatly affect the quality.
Isospin symmetry can be introduced for $u, \bar{u}, d, \bar{d}$:

$$D_{\bar{u}}^{\pi^+} = D_d^{\pi^+} \tag{4.3}$$

and

$$D_{u+\bar{u}}^{\pi^+} = N D_{d+\bar{d}}^{\pi^+} \tag{4.4}$$

as well as

$$D_s^{\pi^+} = D_{\bar{s}}^{\pi^+} = N D_{\bar{u}}^{\pi^+} \tag{4.5}$$

For charged Kaons one needs to fit $D^{K^+}_{s+\bar{s}}$ and $D^{K^+}_{u+\bar{u}}$ independently since a secondary $s\bar{s}$ pairs necessary to form a $|K^+\rangle = |u\bar{s}\rangle$ are not produced as often from up quarks as from $\bar{s}$.
For unfavored fragmentation into Kaons one can also assume that all functions have the same form:

$$D^{K^+}_{s} = D^{K^+}_{\bar{u}} = D^{K^+}_{d} = D^{K^+}_{\bar{d}} \tag{4.6}$$

For heavy quarks the same functional form for D^H_i is used, the only difference is the fact that γ_i can be set to 0 and $D^H_c = D^H_{\bar{c}}$ as well as $D^H_b = D^H_{\bar{b}}$ can be assumed.

4.2 DGLAP Evolution with Mellin Technique

As seen in Chapter 2.3 the convolutions in equations (2.3) and (2.8) turn into products in Mellin space, which reduces the computing time by orders of magnitude.
One has to transform the parametrization (Eq. (4.2)) into mellin space and take the Mellin moments of coefficient and fragmentation functions as well to be able to work completely in mellin space.
Exact coefficient and splitting functions in Mellin space are taken from Refs. [1, 6, 36] and can be found in the Appendix.
One of the biggest challenges in working in Mellin space is the Mellin inversion:

$$D_j^H(z, Q^2) = \frac{1}{2\pi i} \int_C dn z^{-n} D_{jM}^H(n, Q^2) \tag{4.7}$$

, where the contour C runs parallel to the imaginary axis and right of the rightmost pole p_r in the integrand (all poles lie only on the real axis).
The contour should be chosen so that the integral converges most efficiently, to further reduce computational efforts.
Since the integrand is analytic in z, the minimum of the function along the real axis is a saddle point in the complex plane. Along C the integrand stays real, since it is also a contour of stationary phase.
The textbook contour $n = c + iy$ used in Ref. [32] can be modified to fulfill the requirements stated above [29], which leads to the following inversion integral:

$$F(z) = \frac{1}{\pi} \int_0^\infty \mathrm{Im}\left[dn z^{-j} F_{\mathrm{mellin}}(n)\right] \tag{4.8}$$

In our case the contour is $j = p_r + ne^{i\Phi}$, with the rightmost pole being $p_r = 1.3$ and the angle $\Phi = \frac{3}{4}\pi$.
Since the moments become increasingly irrelevant the higher one goes, it is sufficient to let the integral run to a finite point of choice, depending on the desired accuracy and available computing power (in this case 5).
Since the result of this integral needs to be real, the imaginary part of the integrand is used.

This method leads to one purely numerical integral (Eq. (4.8)), computed with the Mathematica-Function "NIntegrate", and significantly less computing time.

4.3 Program

Using Mathematica, a program was compiled, using the parametrization from Eq. (4.2) for D_i^H to perform a DGLAP evolution in Mellin space.
Initially it was attempted to solve the evolution equations numerically without the use of a Mellin transform. The computational effort for solving those numerical integrals turned out to be intangible in Mathematica, which lead to the use of Mellin technique. Then the the total fragmentation function was calculated in Mellin space and finally an inversion was performed.
The next step was calculating the cross section and performing a fit.
When trying to perform a numerical fit in Mathematica several problems were encountered.
The inverse Mellin transform is an integral without an analytic solution, that can either be computed purely numerically or by using an approximation technique that results in a pseudo-analytical result [29].
In Mathematica one has the possibility of using various approximation techniques, none of which produced reasonable results for an integral as complex as the one used in this analysis.
Solving purely numerically, using “NIntegrate”, proved to be successful.
Upon performing the fit, however, various other difficulties were encountered.
Apparently, a purely numerical fit in Mathematica can only be accomplished successfully for fairly simple functions, unlike the ones appearing here. The main problem that had to be faced was the fact that during the fit Mathematica tried to evaluate the function before the parameters necessary for evaluation were available, since they need to be determined through the fit.
The method used most commonly for FF calculations is χ^2, which was also used in this thesis. I decided to start from the parameters determined by Ref. [5], vary them and calculate a χ^2 for each set of parameters.
The parameters corresponding to the lowest χ^2 were then used to compare to the data in a plot.
The variation of $N_i, \alpha_i, \beta_i, \gamma_i$ and δ_i was done randomly within $\pm 100\%$, since any other variation would have either been to time consuming or not take the entire phase space into account, in a fit having to be done by hand like in this case.
After having calculated a certain set of parameters with a sufficiently small χ^2 the agreement with the data was checked in every point separately and followed by a variation of the parameters with most discrepancies to reach maximum convergence.
The full working code can be found in the appendix.

Chapter 5

Results and Discussion

5.1 Leading Order Fits

5.1.1 Pion

The plots for the LO Pion fit can be found in Fig. 5.1 and 5.2.
The cut-off at low z was taken at $z_{\text{min}} = 0.05$ and the parameters determined in this analysis are shown in Tab. 5.1.1

	N	α	β	γ	δ
$(u+\bar{u})$	0.102	-0.144	0.555	10.122	7.969
$(d+\bar{d})$	0.314	-0.144	0.555	10.122	7.969
$(s+\bar{s})$	0.080	0.101	3.039	11.479	12.409
$(c+\bar{c})$	0.476	-0.134	5.923	0.0	0.0
$(b+\bar{b})$	0.308	-0.940	5.923	0.0	0.0
g	0.799	26.766	11.650	-0.323	11.626

Table 5.1: The parameters in the table describe the LO fragmentation function $D_i^{\pi^0}$ (see Eq. (4.2)) of neutral Pions at an input scale of $\mu_0 = 1$ GeV for light quarks and $\mu_0 = 1.43$ GeV and $\mu_0 = 4.3$ GeV corresponding to the masses of charm and bottom quarks

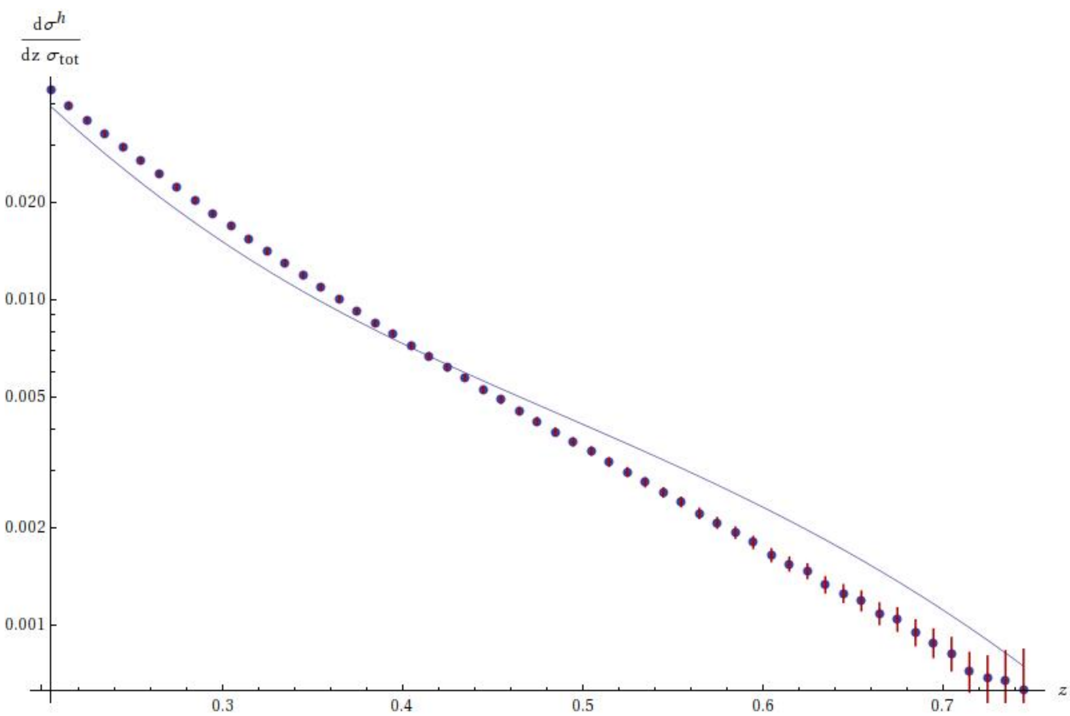

Figure 5.1: LO fit for π^0 plotted against BELLE-data; the solid line represents the cross section calculated in this analysis; the dotted line shows the data points with the experimental errors represented by the red error bars; the values on the z-axis are energy values according to the definitions in Chapter 2; the vertical axis shows the number of hadrons for each energy value z and the area under the curve represents the total hadron multiplicity

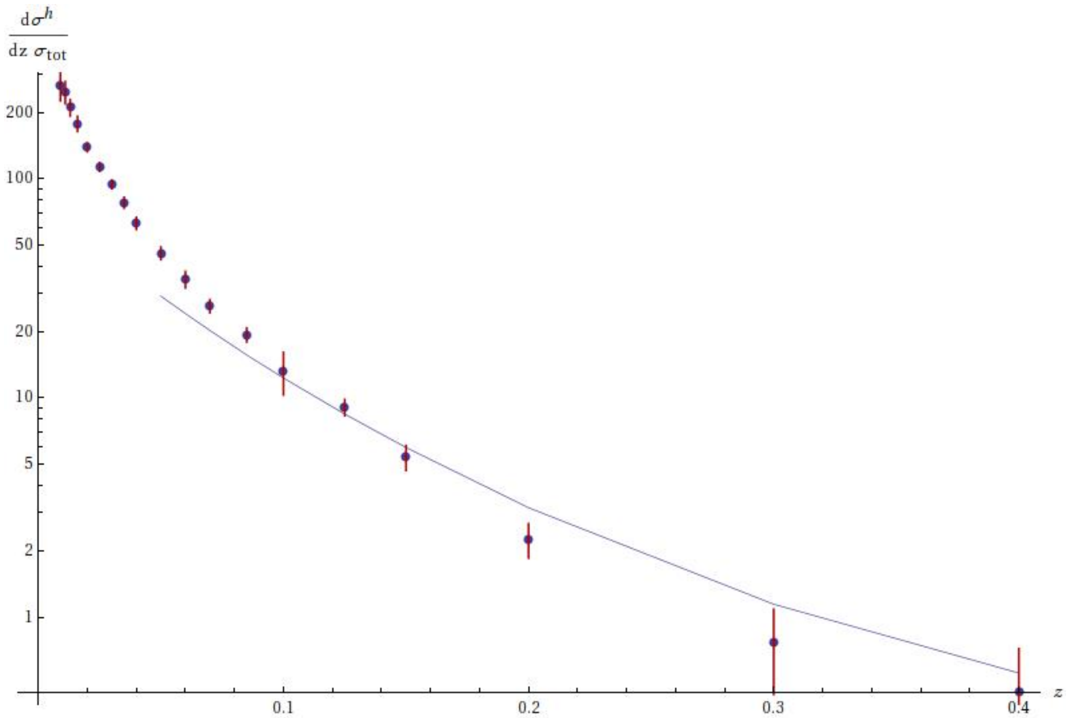

Figure 5.2: LO fit for $\pi 0$ plotted against OPAL-data; the solid line represents the cross section calculated in this analysis; the dotted line shows the data points with the experimental errors represented by the red error bars; the values on the z-axis are energy values according to the definitions in Chapter 2; the vertical axis shows the number of hadrons for each energy value z and the area under the curve represents the total hadron multiplicity

As one can easily see this analysis is not as accurate as the one performed by Ref. [5]. The reason for which most probably lies in the suboptimal fitting procedure, which does not let the fit converge as efficiently as hoped. One can see that the fit is of correct orders of magnitude for BELLE as well as OPAL data, whereas the shape of the curve differs.
For BELLE energies one can observe that the function predicts a harder spectrum with lower yields for the low-z regions and higher yields for high-z.
For OPAL energies the shape of the curve differs quite significantly at low z-regions but is still within the fairly large expected experimental errors.

5.1.2 Kaon

The plots for the LO Kaon fit can be found in Fig. 5.3 and 5.4.
The cut-off at low z was taken at $z_{\text{min}} = 0.1$.

	N	α	β	γ	δ
$(u+\bar{u})$	0.0111	0.809	2.370	10.122	24.816
$(d+\bar{d})$	0.0001	0.376	18.099	3.022	2.615
$(s+\bar{s})$	0.090	1.231	2.215	11.479	25.692
$(c+\bar{c})$	0.017	0.191	0.327	0.0	0.0
$(b+\bar{b})$	0.061	-0.092	11.474	0.0	0.0
g	0.043	7.421	11.650	0.711	0.0

Table 5.2: The parameters in the table describe the LO fragmentation function $D_i^{K^0}$ (see Eq. (4.2)) of neutral Kaons at an input scale of $\mu_0 = 1$ GeV for light quarks and $\mu_0 = 1.43$ GeV and $\mu_0 = 4.3$ GeV corresponding to the masses of charm and bottom quarks

Again, one can see fairly big discrepancies, due to the suboptimal fit procedure.
Another reason for the higher inaccuracy with the Kaon fit could be the fact that the problematic region, the low z-values, sets in earlier due to the larger Kaon mass, which is the reason for raising the cut-off to $z_{\text{min}} = 0.1$. One can therefore get less well constrained fragmentation functions for Kaons.
At Belle energies one can see that the fitted function predicts lower values at low z-regions. The higher predictions at high z-regions is only slightly above the experimental errors.
From the fitted function for OPAL energies one expects a slightly higher total hadron multiplicity than measured in the experiment.

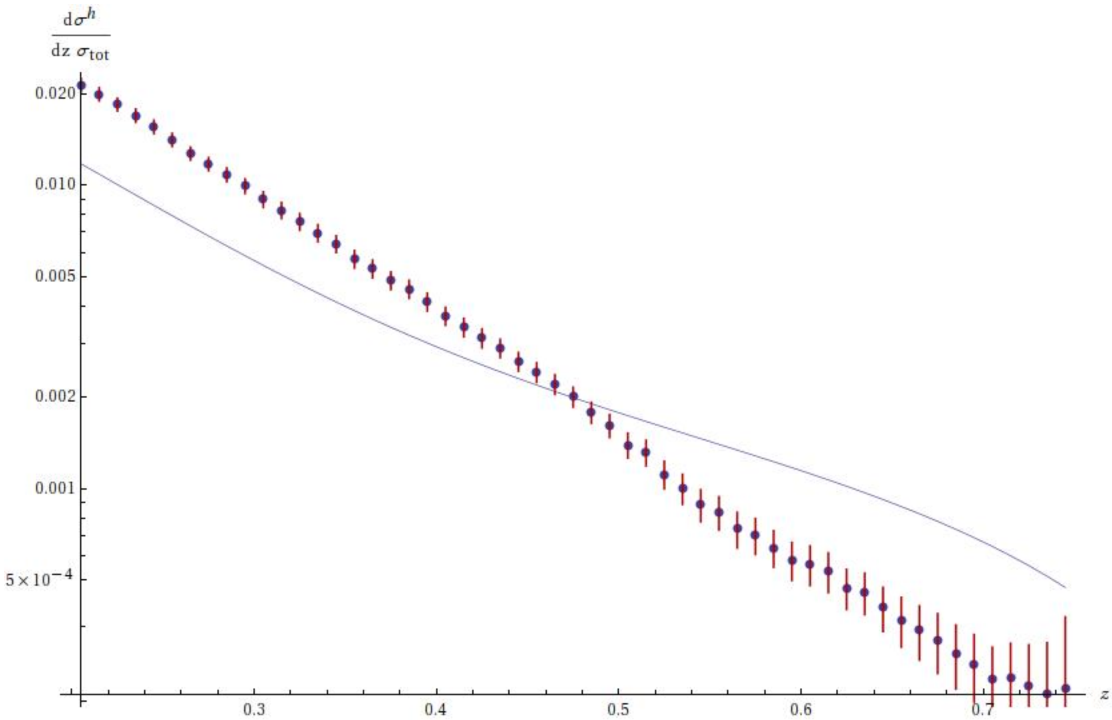

Figure 5.3: LO fit for K^0, to BELLE-data; the solid line represents the cross section calculated in this analysis; the dotted line shows the data points with the experimental errors represented by the red error bars; the values on the z-axis are energy values according to the definitions in Chapter 2; the vertical axis shows the number of hadrons for each energy value z and the area under the curve represents the total hadron multiplicity

Due to the fact that data from only two experiments was used, the determination of the fit parameters is less precise than in analyses comparing a higher number of data sets.
One can also expect better constrained fragmentation functions, in close agreement with experimental data, in the NLO analysis.
As seen in previous analyses one can expect a significant decrease in the total χ^2. The most striking difference can be expected in the gluon fragmentation function, whereas for quarks the differences should be less prominent.
A NLO DGLAP evolution was performed in this analysis and can be found in the code, but the significantly increased complexity of the numerical integral of the Mellin inversion lead to problems in the fitting procedure, that did not allow the fit to converge. Due to the limited informative value of that part of the analysis, the NLO results are omitted here.

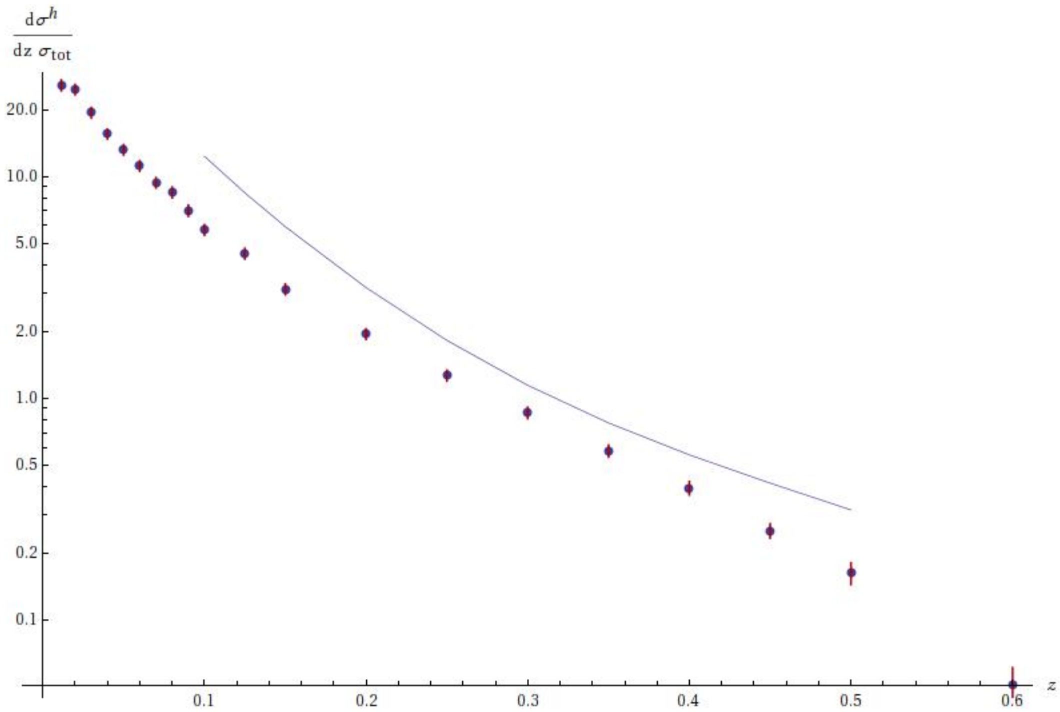

Figure 5.4: LO fit for K^0, to OPAL-data; the solid line represents the cross section calculated in this analysis; the dotted line shows the data points with the experimental errors represented by the red error bars; the values on the z-axis are energy values according to the definitions in Chapter 2; the vertical axis shows the number of hadrons for each energy value z and the area under the curve represents the total hadron multiplicity

5.2 Fragmentation Functions

In this Chapter a comparison between the fragmentation functions $D_i^{\pi^0,K^0}$, calculated in this analysis to the ones obtained in the analysis performed by DSS is shown.
The LO results are compared to the LO and NLO results found by DSS [5]. One can see that the general forms of the fragmentation functions are in fairly good agreement with the ones determined by DSS. The biggest difference can be seen in the height of the functions which could be explained by the fact that in the fit performed in this analysis no constraints between up and down quarks were used. This leads to a different N-parameter, the parameter responsible for the position of the function. Another reason for the discrepancies, especially compared to the NLO results of DSS, could be the difference between LO and NLO as well as the use of only two datasets in the fit.

5.2.1 Pion

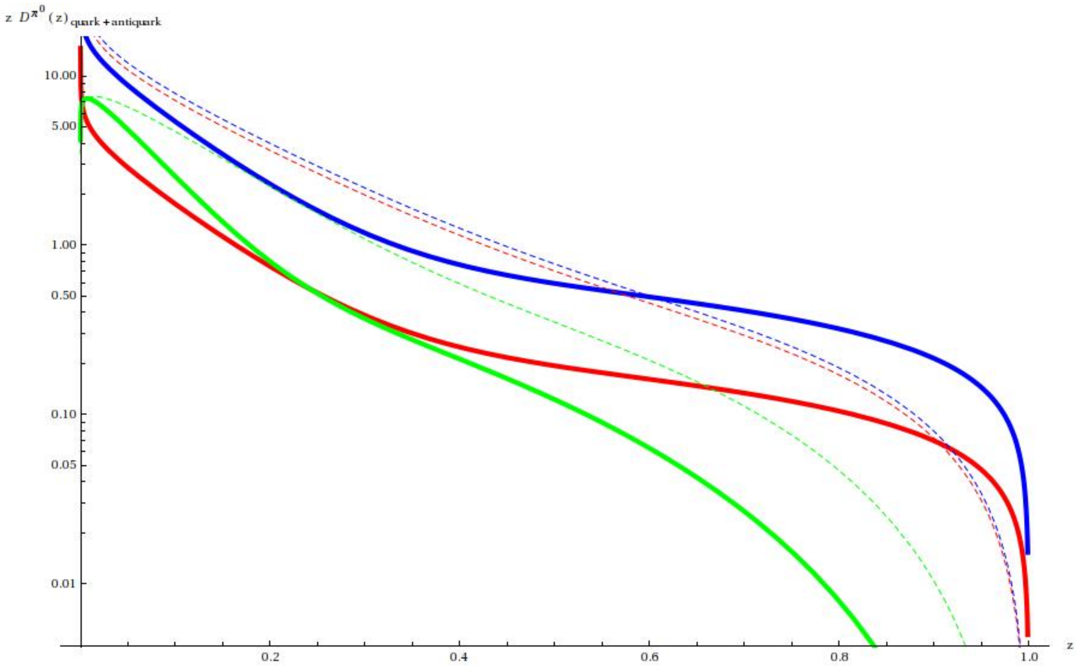

Figure 5.5: This Plot shows the fragmentation functions for Pions from light quarks; the solid lines represent the LO functions calculated with the parameters determined in this analysis, the dashed lines represent the LO functions calculated with parameters determined by DSS [5] $D^{\pi^0}_{u+\bar{u}}$: blue; $D^{\pi^0}_{d+\bar{d}}$: red; $D^{\pi^0}_{s+\bar{s}}$: green

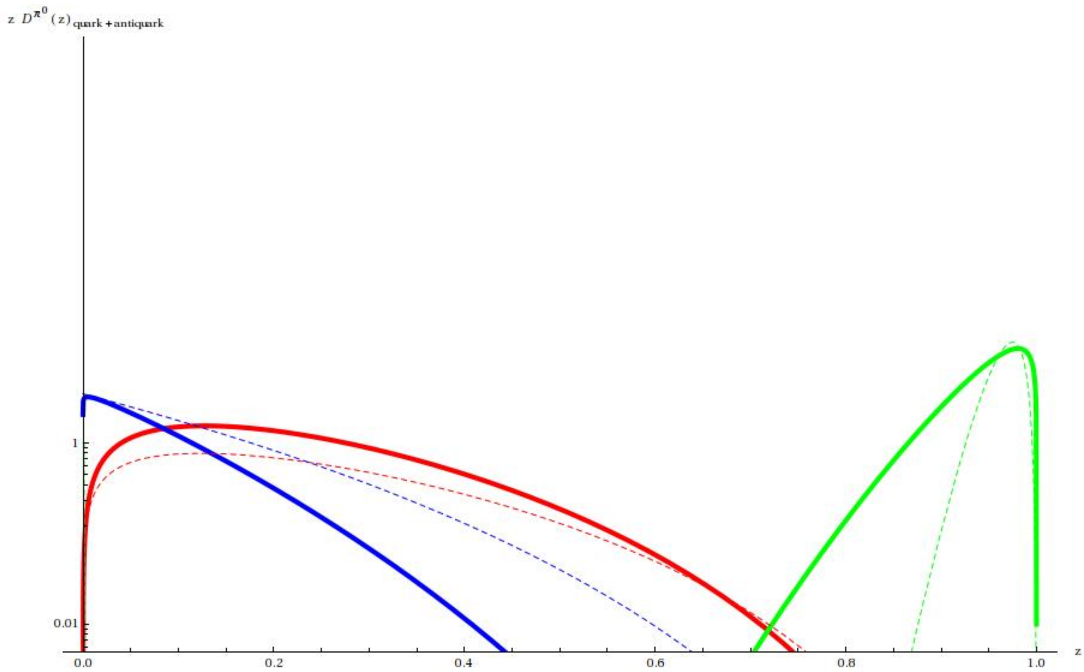

Figure 5.6: This Plot shows the fragmentation functions for Pions from heavier quarks and gluons; the solid lines represent the LO functions calculated with the parameters determined in this analysis, the dashed lines represent the LO functions calculated with parameters determined by DSS [5] $D^{\pi^0}_{c+\bar{c}}$: blue; $D^{\pi^0}_{b+\bar{b}}$: red; $D^{\pi^0}_{g}$: green

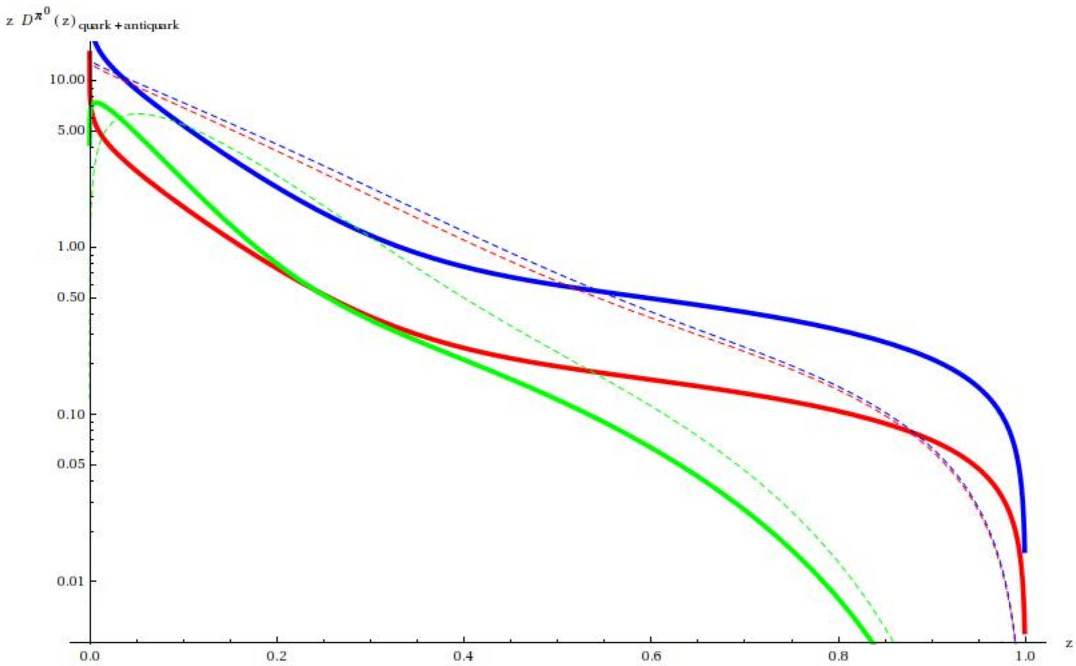

Figure 5.7: This Plot shows the fragmentation functions for Pions from light quarks; the solid lines represent the LO functions calculated with the parameters determined in this analysis, the dashed lines represent the NLO functions calculated with parameters determined by DSS [5] $D^{\pi^0}_{u+\bar{u}}$: blue; $D^{\pi^0}_{d+\bar{d}}$: red; $D^{\pi^0}_{s+\bar{s}}$: green

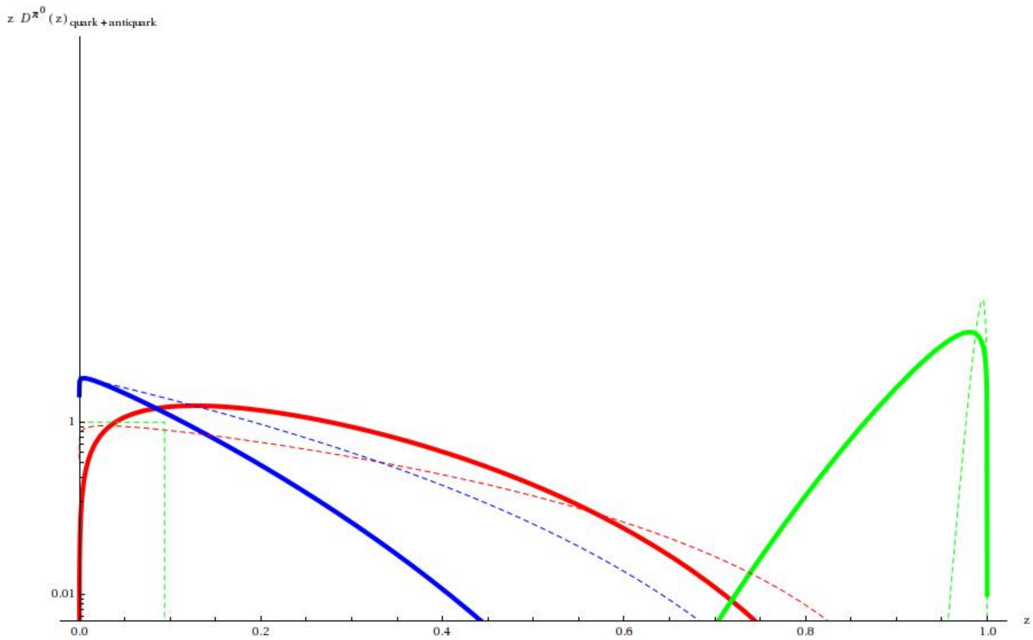

Figure 5.8: This Plot shows the fragmentation functions for Pions from heavier quarks and gluons; the solid lines represent the LO functions calculated with the parameters determined in this analysis, the dashed lines represent the NLO functions calculated with parameters determined by DSS [5] $D^{\pi^0}_{c+\bar{c}}$: blue; $D^{\pi^0}_{b+\bar{b}}$: red; $D^{\pi^0}_{g}$: green

5.2.2 Kaon

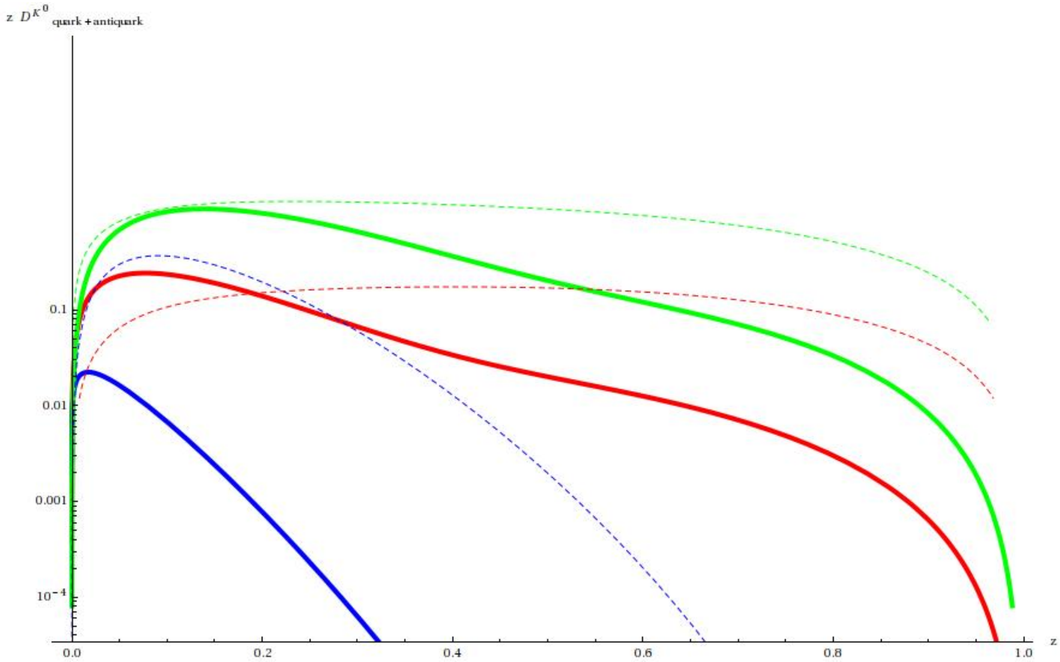

Figure 5.9: This Plot shows the fragmentation functions for Pions from light quarks; the solid lines represent the LO functions calculated with the parameters determined in this analysis, the dashed lines represent the LO functions calculated with parameters determined by DSS [5] $D^{K^0}_{u+\bar{u}}$: blue; $D^{K^0}_{d+\bar{d}}$: red; $D^{K^0}_{s+\bar{s}}$: green

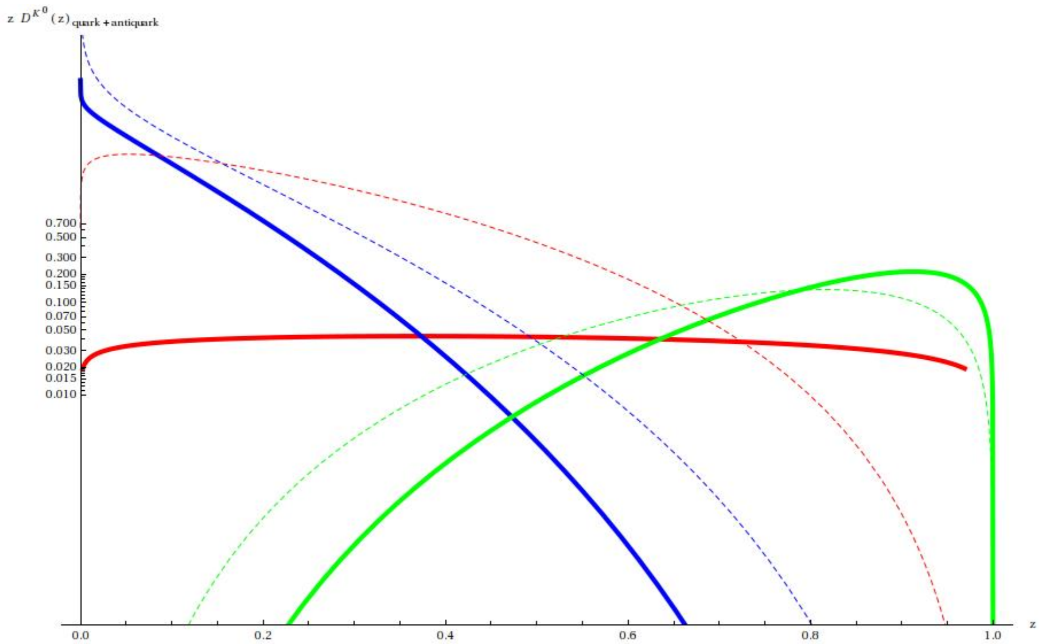

Figure 5.10: This Plot shows the fragmentation functions for Pions from heavier quarks and gluons; the solid lines represent the LO functions calculated with the parameters determined in this analysis, the dashed lines represent the LO functions calculated with parameters determined by DSS [5] $D^{K^0}_{c+\bar{c}}$: blue; $D^{K^0}_{b+\bar{b}}$: red; $D^{K^0}_{g}$: green

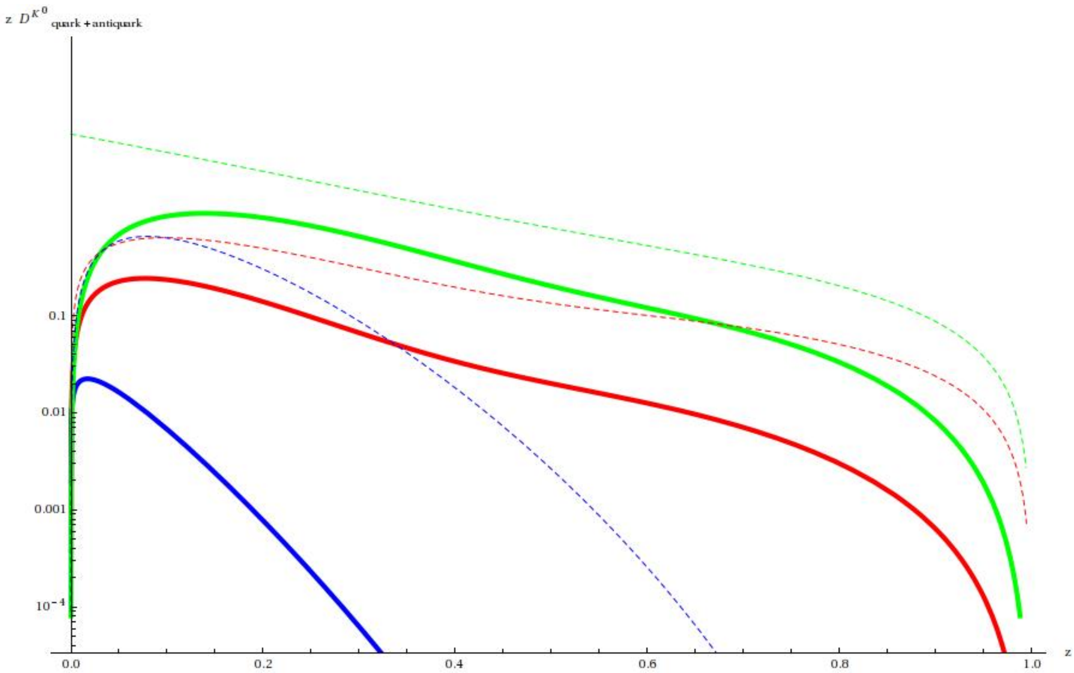

Figure 5.11: This Plot shows the fragmentation functions for Pions from light quarks; the solid lines represent the LO functions calculated with the parameters determined in this analysis, the dashed lines represent the NLO functions calculated with parameters determined by DSS [5] $D^{K^0}_{u+\bar{u}}$: blue; $D^{K^0}_{d+\bar{d}}$: red; $D^{K^0}_{s+\bar{s}}$: green

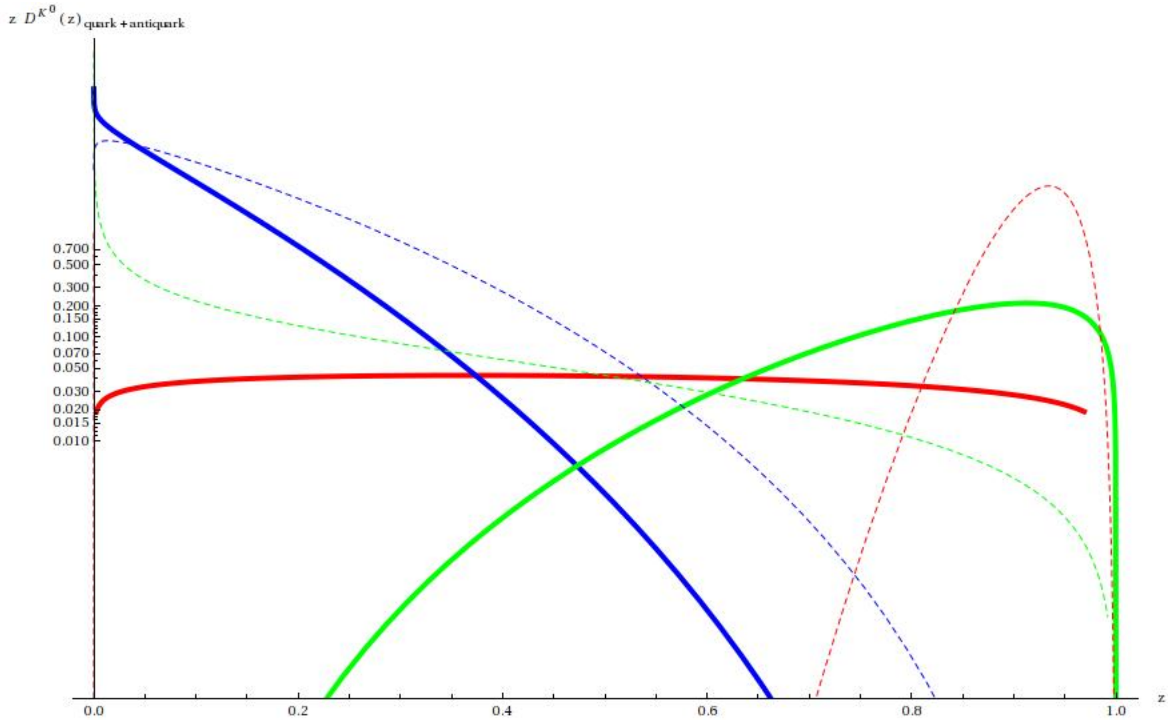

Figure 5.12: This Plot shows the fragmentation functions for Pions from heavier quarks and gluons; the solid lines represent the LO functions calculated with the parameters determined in this analysis, the dashed lines represent the NLO functions calculated with parameters determined by DSS [5] $D^{K^0}_{c+\bar{c}}$: blue; $D^{K^0}_{b+\bar{b}}$: red; $D^{K^0}_{g}$: green

Appendix A

A.1 Renormalization

First developed in perturbative QED, renormalization is a way of treating infinities of a theory, e.g. the ones coming from evaluating Feynman diagrams [37].
Due to the differences between leptons and quarks a different way of renormalization needs to be used in QCD than in QED.
There are various ways to remove divergencies in non-abelian gauge theories, out of which the most commonly and successfully used is the method of dimensional regularization and renormalization, the so called $\bar{MS}$-scheme (Modified Minimal Subtraction-scheme).
One first calculates Dirac algebra and momentum integrals in n dimensions and then continues these calculations analytically continued to four dimensions.
Ultraviolet and infrared divergencies that originate from the Γ-function, then turn into poles in $\epsilon = n - 4$.
There are multiple ways of performing a dimensional regularization, where the differences lie in the definition of the Dirac matrices.
The MS-scheme absorbs infinities coming from perturbative calculations into counterterms, where in the $\bar{MS}$-scheme one absorbs the divergent terms plus a universal constant, that always comes from the calculation of Feynman diagrams, along with the divergencies.
In the latter one only needs to eliminate the $\frac{1}{\epsilon}$ of the Green functions and the renormalization constants appear in the Lagrangian.
It is clear the one needs renormalization invariance in order to be able to use a renormalization scheme in a useful manner, which means that all physical observable need to be the same, independent of the renormalization scheme used.
A differential approach became important when the momentum dependence

of the QED coupling constant, due to the renormalized charge was discovered.

One can renormalize in two different schemes, say R_1 and R_2. The operation, that relates quantities of two different renormalization schemes is a transformation from R_1 to R_2, the group of which is called the renormalization group.

Invariance under this group is used to investigate the asymptotic behavior of Green functions with the Renormalization Group Equation (see Eq. (2.12)). (Details see Ref. [37, 38])

A.2 Functions

Splitting Functions in Mellin Space

In a Fragmentation Function z represents a fraction of the partons momentum carried by the hadron. When QCD corrections are taken into account one observes a scale dependence z-distribution.
A change in a FF $D_i^H(z, Q^2)$ with an increase in the scale Q^2 occurs through the splitting or a parton of type i into type j [25, 27, 36].
The Splitting Function is then P_{ji} rather than P_{ij} since the D_j^H represents the FF of the final parton (see Eq. (2.8) and (2.9)) [8].

LO

$$P_{qq}(j) = C_F\left(-\frac{1}{2} + \frac{1}{j(j+1)} - S_2(j)\right) \tag{A.1}$$

$$P_{qg}(j) = T_f\left(\frac{(2+j+j^2)}{j(j+1)(j+2)}\right) \tag{A.2}$$

$$P_{gq}(j) = C_F\left(\frac{2+j+j^2}{j(j^2-1)}\right) \tag{A.3}$$

$$P_{gg}(j) = 2C_A\left(-\frac{1}{12} + \frac{1}{j(j-1)} + \frac{1}{(j+1)(j+2)} - S_1(j)\right) \tag{A.4}$$

$$\tag{A.5}$$

$C_A = 3$, $C_F = \frac{4}{3}$ and $T_f = \frac{1}{2}$ are constants acc.t. Refs. [1, 6, 21].

NLO

$$
\begin{aligned}
P_{qq}\left(j,Q^2\right) \quad = \quad & -\frac{\gamma^s_{qq}\left(j\right)}{8} + C_F^2 \\
& \left(-4S_1\left(j\right) + 3 + \frac{2}{j\left(j+1\right)}\right) \\
& \left(2S_2\left(j\right) - \frac{\pi^2}{3} - \frac{2j+1}{j^2\left(j+1\right)}\right) + \\
& C_F T_F \left(\frac{80}{9}\frac{1}{j-1} + \frac{8}{j^3} + \frac{12}{j^2} - \frac{12}{j} + \frac{8}{\left(j+1\right)^3} + \right. \\
& \left. \frac{28}{\left(j+1\right)^2} - \frac{4}{j+1} + \frac{32}{3}\frac{1}{\left(j+2\right)^2} + \frac{224}{9}\frac{1}{j+2}\right)
\end{aligned}
\tag{A.6}
$$

$$
\begin{aligned}
P_{qg}\left(j,Q^2\right) \quad = \quad & \frac{1}{f}\left(T_F^2\frac{8}{3}\right. \\
& \left(S_1\left(j+1\right)\frac{j^2+j+2}{j\left(j+1\right)\left(j+2\right)} + \frac{1}{j^2} - \frac{5}{3}\frac{1}{j} - \frac{1}{j\left(j+1\right)}\right. \\
& \left. -\frac{2}{\left(j+1\right)^2} + \frac{4}{3}\frac{1}{j+1} + \frac{4}{\left(j+2\right)^2} - \frac{4}{3}\frac{1}{j+2}\right) + \\
& C_F T_F \left(\left(-2S_1\left(j+1\right)^2 + S_1\left(j+1\right) + 10S_2\left(j+1\right)\right)\right. \\
& \frac{j^2+j+2}{j\left(j+1\right)\left(j+2\right)} + 4S_1\left(j+1\right) \\
& \left(-\frac{1}{j^2} + \frac{1}{j} + \frac{1}{j\left(j+1\right)} + \frac{2}{\left(j+1\right)^2} - \frac{4}{\left(j+2\right)^2}\right) \\
& -\frac{2}{j^3} + \frac{5}{j^2} - \frac{12}{j} + \frac{4}{j^2\left(j+1\right)} - \frac{12}{j\left(j+1\right)^2} - \frac{6}{j\left(j+2\right)} \\
& \left. +\frac{4}{\left(j+1\right)^3} - \frac{4}{\left(j+1\right)^2} + \frac{23}{j+1} - \frac{20}{j+2}\right) C_A T_F \\
& \left(\left(2S_1\left(j+1\right)^2 - \frac{10}{3}S_1\left(j+1\right) - 6S_2\left(j+1\right) + G\left(j+1\right) + \pi^2\right)\right. \\
& \frac{j^2+j+2}{j\left(j+1\right)\left(j+2\right)} - 4S_1\left(j+1\right)\left(-\frac{2}{j^2} + \frac{1}{j} + \frac{1}{j\left(j+1\right)} + \frac{4}{\left(j+1\right)^2}\right. \\
& \left. - \frac{6}{\left(j+2\right)^2}\right) - \frac{40}{9}\frac{1}{j-1} + \frac{4}{j^3} + \frac{8}{3}\frac{1}{j^2} + \frac{26}{9}\frac{1}{j} - \frac{8}{j^2\left(j+1\right)^2} \\
& +\frac{22}{3}\frac{1}{j\left(j+1\right)} + \frac{16}{\left(j+1\right)^3} + \frac{68}{3}\frac{1}{\left(j+1\right)^2} - \frac{190}{9}\frac{1}{j+1} + \\
& \left.\left. \frac{8}{\left(j+1\right)^2\left(j+2\right)} - \frac{4}{\left(j+2\right)^2} + \frac{356}{9}\frac{1}{j+2}\right)\right)
\end{aligned}
\tag{A.7}
$$

$$
\begin{aligned}
P_{gq}\left(j,Q^2\right) \;=\;& 2f\left(C_F^2\left(\left(\left(S_1\left(j\right)^2-3S_2\left(j\right)-\frac{2\pi^2}{3}\right)\frac{j^2+j+2}{\left(j-1\right)j\left(j+1\right)}+2S_1\left(j\right)\right.\right.\right.\\
&\left(\frac{4}{\left(j-1\right)^2}-\frac{2}{\left(j-1\right)j}-\frac{4}{j^2}+\frac{3}{\left(j+1\right)^2}-\frac{1}{j+1}\right)\\
&-\frac{8}{\left(j-1\right)^2j}+\frac{8}{\left(j-1\right)j^2}+\frac{2}{j^3}+\frac{8}{j^2}-\frac{1}{2j}+\frac{1}{\left(j+1\right)^3}\\
&\left.-\frac{5}{2}\frac{1}{\left(j+1\right)^2}+\frac{9}{2}\frac{1}{j+1}\right)C_FC_A\left(\left(-S_1\left(j\right)+5S_2\left(j\right)-G\left(j\right)+\frac{\pi^2}{6}\right)\right.\\
&\frac{j^2+j+2}{\left(j-1\right)j\left(j+1\right)}+2S_1\left(j\right)\left(-\frac{2}{\left(j-1\right)^2}+\frac{2}{\left(j-1\right)j}+\frac{2}{j^2}-\frac{2}{\left(j+1\right)^2}\right.\\
&\left.+\frac{1}{j+1}\right)-\frac{8}{\left(j+1\right)^3}+\frac{6}{\left(j+1\right)^2}+\frac{17}{9}\frac{1}{j-1}+\frac{4}{\left(j-1\right)^2j}\\
&-\frac{12}{\left(j-1\right)j^2}-\frac{8}{j^2}+\frac{5}{j}-\frac{2}{j^2\left(j+1\right)}\\
&\left.\left.-\frac{2}{\left(j+1\right)^3}-\frac{7}{\left(j+1\right)^2}-\frac{1}{j+1}-\frac{8}{3}\frac{1}{\left(j+2\right)^2}-\frac{44}{9}\frac{1}{j+2}\right)\right)
\end{aligned}
\tag{A.8}
$$

$$
\begin{aligned}
P_{gg}\left(j,Q^2\right) \;=\;& -\frac{\gamma_{gg}^s\left(j\right)}{8}+C_FT_F\left(-\frac{16}{3}\frac{1}{\left(j-1\right)^2}+\frac{80}{9}\frac{1}{j-1}+\right.\\
&\frac{8}{j^3}-\frac{16}{j^2}+\frac{12}{j}+\frac{8}{\left(j+1\right)^3}-\frac{24}{\left(24\right)^2}+\frac{4}{j+1}-\frac{16}{3}\frac{1}{\left(j+1\right)^2}\\
&\left.-\frac{224}{9}\frac{1}{j+2}\right)+C_AT_F\left(-\frac{8}{3}\right)\left(S_2\left(j\right)-\frac{1}{\left(j-1\right)^2}+\frac{1}{j^2}-\frac{1}{\left(j+1\right)^2}\right.\\
&\left.+\frac{1}{\left(j+2\right)^2}-\frac{\pi^2}{6}\right)+C_A^2\left(-8S_1\left(j\right)S_2\left(j\right)+8S_1\left(j\right)\right.\\
&\left(\frac{1}{\left(j-1\right)^2}-\frac{1}{j^2}+\frac{1}{\left(j+1\right)^2}-\frac{1}{\left(j+2\right)^2}+\frac{\pi^2}{6}\right)\\
&+\left(8S_2\left(j\right)-\frac{4\pi^2}{3}\right)\left(\frac{1}{j-1}-\frac{1}{j}+\frac{1}{j+1}-\frac{1}{j+2}+\frac{11}{12}\right)-\\
&\frac{8}{\left(j-1\right)^3}+\frac{22}{3}\frac{1}{\left(j-1\right)^2}-\frac{8}{\left(j-1\right)^2j}-\frac{8}{\left(j-1\right)j^2}-\frac{8}{j^3}-\\
&\frac{14}{3}\frac{1}{j^2}-\frac{8}{\left(j+1\right)^3}+\frac{14}{3}\frac{1}{\left(j+1\right)^2}-\frac{8}{\left(j+1\right)^2\left(j+2\right)}\\
&\left.-\frac{8}{\left(j+1\right)\left(j+2\right)^2}-\frac{8}{\left(j+2\right)^3}-\frac{22}{3}\frac{1}{\left(j+2\right)^2}\right)
\end{aligned}
\tag{A.9}
$$

The functions S_1 and S_2 are defined as

$$S_1(j) = 0.577216 + \log(\Gamma(j+1)) \tag{A.10}$$

$$S_2(j) = \frac{\pi^2}{6} + \frac{1}{(1+j)\log[\Gamma(1+j)]} - \frac{\log(1+j)\Psi(0,1+j)}{\log(1+j)^2} \tag{A.11}$$

in Mellin space. Γ is the Euler Gamma function and Ψ the digamma function, with $G(j+1)$ being a function combining Γ and Ψ.
The $\gamma_{ij}s$ are the singlet splitting functions, that take into account a quark of flavor i fragmenting into another quark of flavor i [1, 6, 21].

Coefficient Functions in Mellin Space

Coefficient functions are probabilities of creating a parton i with a certain fraction of the beam energy and are in Leading Order simply given by the Yukawa couplings for the particle in question.
In NLO, in mellin space they take following form [1, 6]:

$$\begin{aligned}
C_1^q(j) &= C_F\left(5S_1(j) + S_2(j)^2 + S_1(j)\left(\frac{3}{2} - \frac{1}{j(j+1)}\right)\right. \\
&\quad \left. -\frac{2}{j^2} + \frac{3}{(j+1)^2} - \frac{3}{2}\frac{1}{j+1} - \frac{9}{2} + \left(\frac{1}{j(j+1)}\right)\right) \\
C_1^g(j) &= 2C_F\left(-S_1(j)\frac{j^2+j+2}{(j-1)j(j+1)} - \frac{4}{(j-1)^2} + \frac{4}{j^2} - \frac{3}{(j+1)^2}\right) \\
&\quad +2\frac{j^2+j+2}{j(j^2-1)} \\
C_L^q(j) &= C_F\frac{1}{j} \\
C_L^g(j) &= C_F\frac{4}{(j-1)j}
\end{aligned} \tag{A.12}$$

A.3 Abbreviations

DGLAP Evolution Dokshitzer–Gribov–Lipatov–Altarelli–Parisi Evolution Equations

DSS DeFlorian-Stratmann-Sassot Analysis Group

FF Fragmentation Function

HKNS Hirai-Kumano-Nagai-Sudoh Analysis Group

KKP Kniehl-Kramer-Poetter Analysis Group

LO Leading Order

NLO Next-To-Leading Order

PDF Parton Distribution Function

pQCD perturbative Quantum Chromodynamics

QCD Quantum Chromodynamics

SIDIS Semi Inclusive Deep Inelastic Scattering

A.4 Code

On the following pages the working code with example-data and resulting plots can be found.

(*Fragmentation Functions*)

(*

Step 1: Defnninitions

define functional form $D^H{}_j$
Energies relevant for DGLAP evolution
running coupling constant α_S
splitting functions P_{ij}
coefficient functions C_i

(*

Step 2: DGLAP evolution
convolution of fragmentation function with splitting functions: $D_P = \frac{d\, D^H{}_j}{d\ \ln Q^2} = \Sigma_i \int_0^1 P_{ij}\left(\frac{z}{\xi}, Q^2\right) D^H{}_i\left(\xi, Q^2\right) \frac{d\xi}{\xi}$
*)

(*

Step 3: Calculation of cross section
convolution of $D_P = \frac{d\, D^H{}_j}{d\ \ln Q^2}$ with coefficient functions C_i similarly to DGLAP evolution
calculating cross section

IN MELLIN SPACE:

Step I: Definitions in Mellin space
define functional form $D^H{}_{j_{mellin}}$
splitting functions $P_{ij_{mellin}}$
coefficient functions $C_{i_{mellin}}$

Step II: DGLAP Evolution
convolution of P_{ij} and $D^H{}_j$ turns into produc: $P_{ij_{mellin}} * D^H{}_{j_{mellin}} = D_{P_{mellin}}$

Step III:
convolutions between C_i and D_P turns into product of $C_{i_{mellin}} * D_{P_{mellin}} =$
D_{C1} and D_{CL} respectively

Step IV: inverse mellin transform
invert $D_{C1}\left(j, Q^2\right)$ and $D_{CL}\left(j, Q^2\right)$ from Mellin space back into $F_1{}^H\left(z, Q^2\right)$ and $F_L{}^H\left(z, Q^2\right)$

Step 5:
calculation of cross section and fit

*)

(*Step 1: Definitions*)

(*functional form*)

$$d[z\_, n\_, \alpha\alpha\ \_, \beta\ \_, \gamma\ \_, \delta\ \_] := \frac{n * z^{\alpha\alpha} * (1 - z)^{\beta} \left(1 + \gamma\, (1 - z)^{\delta}\right)}{\mathrm{Beta}[2 + \alpha\alpha, \beta + 1] + \gamma * \mathrm{Beta}[2 + \alpha\alpha, \beta + \delta + 1]};$$

(*Energies relevant*)

```
BELLE = 10.58^2;
OPAL = 91.5^2;
```

(*Fragmentation Functions*)

(*

Step 1: Defnninitions

define functional form $D^H{}_j$
Energies relevant for DGLAP evolution
running coupling constant α_S
splitting functions P_{ij}
coefficient functions C_i

(*

Step 2: DGLAP evolution
convolution of fragmentation function with splitting functions: $D_P = \frac{d\ D^H{}_j}{d\ \ln\ Q^2} = \Sigma_i \int_0^1 P_{ij}\left(\frac{z}{\xi}, Q^2\right) D^H{}_i\left(\xi, Q^2\right) \frac{d\xi}{\xi}$
*)

(*

Step 3: Calculation of cross section
convolution of $D_P = \frac{d\ D^H{}_j}{d\ \ln\ Q^2}$ with coefficient functions C_i similarly to DGLAP evolution
calculating cross section

IN MELLIN SPACE:

Step I: Definitions in Mellin space
define functional form $D^H{}_{j_{mellin}}$
splitting functions $P_{ij_{mellin}}$
coefficient functions $C_{i_{mellin}}$

Step II: DGLAP Evolution
convolution of P_{ij} and $D^H{}_j$ turns into produc: $P_{ij_{mellin}} * D^H{}_{j_{mellin}} = D_{P_{mellin}}$

Step III:
convolutions between C_i and D_P turns into product of $C_{i_{mellin}} * D_{P_{mellin}} =$
D_{C1} and D_{CL} respectively

Step IV: inverse mellin transform
invert $D_{C1}\left(j, Q^2\right)$ and $D_{CL}\left(j, Q^2\right)$ from Mellin space back into $F_1{}^H\left(z, Q^2\right)$ and $F_L{}^H\left(z, Q^2\right)$

Step 5:
calculation of cross section and fit

*)

(*Step 1: Definitions*)

(*functional form*)

$$d[z\_, n\_, \alpha\alpha\_, \beta\_, \gamma\_, \delta\_] := \frac{n * z^{\alpha\alpha} * (1 - z)^{\beta} \left(1 + \gamma\ (1 - z)^{\delta}\right)}{\text{Beta}[2 + \alpha\alpha, \beta + 1] + \gamma * \text{Beta}[2 + \alpha\alpha, \beta + \delta + 1]};$$

(*Energies relevant*)
BELLE = 10.58^2;
OPAL = 91.5^2;

```
(*running coupling*)
quarkmass = {0.001, 0.004, 0.8, 1.11, 4.1, 170.1}^2;
flav[Q_] := (ftemp = 0;
  For[i = 1, i ≤ Length[quarkmass], i++,
   If[Q ≥ quarkmass[[i]], ftemp += 1];
  ];
  ftemp)
order = 1 (*LO, 2 for NLO*);
lambdavalues = {{0.232, 0.220, 0.153}, {0.248, 0.334, 0.334, 0.131}};
Λ[Q_] := lambdavalues[[order, flav[Q] - 2]];
```

$$\beta 0[Q\_] := 11 - \frac{2\,\mathrm{flav}[Q]}{3};$$

$$\beta 1[Q\_] := 102 - \frac{38\,\mathrm{flav}[Q]}{3};$$

$$l[Q\_] := \left(\frac{1}{\Lambda[Q]}\right)^2;$$

$$\alpha[Q\_] := 4\,\mathrm{Pi}\left(\frac{1}{\beta 0[Q]\,\mathrm{Log}\left[Q \big/ (\Lambda[Q])^2\right]} - \frac{\beta 1[Q]}{(\beta 0[Q])^3}\,\frac{\mathrm{Log}\left[\mathrm{Log}\left[Q \big/ (\Lambda[Q])^2\right]\right]}{\left(\mathrm{Log}\left[Q \big/ (\Lambda[Q])^2\right]\right)^2}\right);$$

```
(*constants and functions necessary for the
 definition coefficient functions and splitting functions*)
cA = 3;
```

$$cF = \frac{4}{3};$$

$$Tf = \frac{1}{2};$$

```
(*Mellin Moments*)
```

$$\psi 1[j\_] := D\left[\mathrm{Log}\left[\mathrm{Gamma}\left[\frac{tempj + 1}{2}\right]\right], tempj\right] /.\ tempj \to j;$$

$$\psi 2[j\_] := D\left[\mathrm{Log}\left[\mathrm{Gamma}\left[\frac{tempj}{2}\right]\right], tempj\right] /.\ tempj \to j;$$

$$\psi 3[j\_] := D[\mathrm{Log}[\mathrm{Gamma}[tempj + 1], tempj + 1]] /.\ tempj \to j;$$

$$tempg = D[(\psi 1[j] - \psi 2[j]), j];$$

$$G[j\_] := -\frac{1}{4}\,\mathrm{PolyGamma}\left[1, \frac{j}{2}\right] + \frac{1}{4}\,\mathrm{PolyGamma}\left[1, \frac{1 + j}{2}\right];$$

$$(*S[[i]][j\_]:=\mathrm{Sum}\left[\frac{1}{j^k},\{k,1,i\}\right];*)$$

$$S1[j\_] := 0.577216 + \psi 3[j];$$

$$(*temp=D[\psi 3[j],j]*)$$

$$S2[j\_] := \frac{\mathrm{Pi}^2}{6} + \frac{1}{(1 + j)\,\mathrm{Log}[\mathrm{Gamma}[1 + j]]} - \frac{\mathrm{Log}[1 + j]\,\mathrm{PolyGamma}[0, 1 + j]}{\mathrm{Log}[\mathrm{Gamma}[1 + j]]^2}(*=temp*);$$

$$(*temp1=D[D[\psi 3[j],j],j]*)$$

$$\text{S3[j\_]} := 1.202057 + -\frac{1}{(1+j)^2\,\text{Log[Gamma[1+j]]}} - \frac{2\,\text{PolyGamma[0, 1+j]}}{(1+j)\,\text{Log[Gamma[1+j]]}^2} + \frac{2\,\text{Log[1+j] PolyGamma[0, 1+j]}^2}{\text{Log[Gamma[1+j]]}^3} - \frac{\text{Log[1+j] PolyGamma[1, 1+j]}}{\text{Log[Gamma[1+j]]}^2};$$

$$(*S_2{}'=*)\,\text{s2[j\_]} := 2 * \text{Sum}\left[\frac{1+(-1)^k}{k^2}, \{k, 1, 2\}\right];$$

$$(*S_3{}'=*)\,\text{s3[j\_]} := 4 * \text{Sum}\left[\frac{1+(-1)^k}{k^3}, \{k, 1, 3\}\right];$$

$$(*\tilde{S}=*)\,\text{ss[j\_]} := \text{Sum}\left[\frac{(-1)^k\,(0.577216 + \psi\,3[j])}{k^2}, \{k, 1, 1\}\right];$$

(*Coefficient Functions*)

$$\text{C1q[j\_]} := \text{cF}\left(5\,\text{S2[j]} + \text{S1[j]}^2 + \text{S1[j]}\left(\frac{3}{2} - \frac{1}{j\,(j+1)}\right) - \frac{2}{j^2} + \frac{3}{(j+1)^2} - \frac{3}{2}\,\frac{1}{j+1} - \frac{9}{2} + \left(\frac{1}{j\,(j+1)} - 2\,\text{S1[j]} + \frac{3}{2}\right)\right);$$

$$\text{C1g[j\_]} := 2\,\text{cF}\left(-\text{S1[j]}\,\frac{j^2+j+2}{(j-1)\,j\,(j+1)} - \frac{4}{(j-1)^2} + \frac{4}{j^2} - \frac{3}{(j+1)^2}\right) + 2\,\frac{j^2+j+2}{j\,\left(j^2-1\right)};$$

$$\text{CLq[j\_]} := \text{cF}\,\frac{1}{j};$$

$$\text{CLg[j\_]} := \text{cF}\,\frac{4}{(j-1)\,j};$$

(*Splitting Functions LO*)

$$\text{Pqq[j\_]} := \text{cF}\left(-\frac{1}{2} + \frac{1}{j\,(j+1)} - \text{S2[j]}\right);$$

$$\text{Pqg[j\_]} := \text{Tf}\left(\frac{\left(2+j+j^2\right)}{j\,(j+1)\,(j+2)}\right);$$

$$\text{Pgq[j\_]} := \text{cF}\left(\frac{\left(2+j+j^2\right)}{j\,\left(j^2-1\right)}\right);$$

$$\text{Pgg[j\_]} := 2\,\text{cA}\left(-\frac{1}{12} + \frac{1}{j\,(j-1)} + \frac{1}{(j+1)\,(j+2)} - \text{S1[j]}\right);$$

(*Splitting Functions NLO*)

$$\gamma\,\text{sNS[j\_]} := \text{cF}^2\left(\frac{16\,\text{S1[j]}\,(2\,j+1)}{j^2\,(j+1)} + 16\left(2\,\text{S1[j]} - \frac{1}{j\,(j-1)}\right)(\text{S2[j]} - \text{s2[j]}) + 24\,\text{S2[j]} + 64\,\text{ss[j]} - 28\,\text{s3[j]} - 3 - \frac{8\left(1+4\,j+5\,j^2+3\,j^3\right)}{j^3\,(j+1)^3}\right) +$$

$$\mathrm{cA}*\mathrm{cF}\left(\frac{536}{9}\,\mathrm{S1}[j]-8\left(2\,\mathrm{S1}[j]-\frac{1}{j\,(j+1)}\right)(2\,\mathrm{S2}[j]-\mathrm{s2}[j])-\frac{88}{3}\,\mathrm{S2}[j]-28\,\mathrm{ss}[j]-\frac{17}{3}-\frac{4}{9}\,\frac{\left(-33+52\,j+236\,j^2+151\,j^3\right)}{j^2\,(j+1)^3}\right)+$$

$$\mathrm{cF}*\mathrm{Tf}\left(-\frac{160}{9}\,\mathrm{S1}[j]+\frac{32}{3}\,\mathrm{S2}[j]+\frac{4}{3}+\frac{16}{9}\,\frac{\left(11\,j^2+5\,j-3\right)}{j^2\,(j+1)^2}\right);$$

$$\gamma\,\mathrm{sqq}[j\_]:=\gamma\,\mathrm{sNS}[j]-16\,\mathrm{cF}*\mathrm{Tf}\left(\frac{\left(5\,j^5+32\,j^4+49\,j^3+38\,j^2+28\,j+8\right)}{(j-1)\,j^3\,(j+1)^3\,(j+2)^2}\right);$$

$$\gamma\,\mathrm{sqg}[j\_]:=$$

$$-8\,\mathrm{cF}*\mathrm{Tf}\left(\frac{\left(4+8\,j+15\,j^2+26\,j^3+11\,j^4\right)}{j^3\,(j+1)^3\,(j+2)}-\frac{4\,\mathrm{S1}}{j^4}+\frac{\left(2+j+j^2\right)\left(5+2\,\mathrm{S1}[j]^2-2\,\mathrm{S2}[j]\right)}{j\,(j+1)\,(j+2)}\right)-$$

$$8\,\mathrm{cA}*\mathrm{Tf}\left(2\left(16+64\,j+104\,j^2+128\,j^3+84\,j^4+36\,j^5+25\,j^6+15\,j^7+6\,j^8+j^9\right)\left((j-1)\,j^3\,(j+1)^3\,(j+2)^3\right)^{-1}+\frac{8\,(3+2\,j)\,\mathrm{S1}[j]}{(j+1)^2\,(j+2)^2}+\frac{\left(2+j+j^2\right)\left(-2\,\mathrm{S1}[j]^2+2\,\mathrm{S2}[j]-2\,\mathrm{s2}[j]\right)}{j\,(j+1)\,(j+2)}\right);$$

$$\gamma\,\mathrm{sgq}[j\_]:=-\frac{32}{3}\,\mathrm{cF}*\mathrm{Tf}\left(\frac{1}{(j+1)^2}+\frac{\left(2+j+j^2\right)\left(-\frac{8}{3}+\mathrm{S1}[j]\right)}{(j-1)\,j\,(j+1)}\right)-$$

$$4\,\mathrm{cF}^2\left(-\frac{\left(-4-12\,j-j^2+28\,j^3+43\,j^4+30\,j^5+12\,j^6\right)}{(j-1)\,j^3\,(j+1)^3}-\frac{4\,\mathrm{S1}[j]}{(j+1)^2}+\frac{\left(2+j+j^2\right)\left(10\,\mathrm{S1}[j]-2\,\mathrm{S2}[j]^2-2\,\mathrm{S2}[j]\right)}{(j-1)\,j\,(j+1)}\right)-$$

$$8\,\mathrm{cA}*\mathrm{cF}\left(\frac{\left(144+432\,j-152\,j^2-1304\,j^3-103\,j^4+695\,j^5\right)}{9\,(j-1)^2\,j^3\,(j+1)^3\,(j+2)^3}+\frac{\left(1678\,j^6+1400\,j^7+621\,j^8+109\,j^9\right)}{9\,(j-1)^2\,j^3\,(j+1)^3\,(j+2)^2}-\frac{\left(-12-22\,j+41\,j^2+17\,j^4\right)\mathrm{S1}[j]}{3\,(j-1)^2\,j^2\,(j+1)}+\frac{\left(2+j+j^2\right)\left(\mathrm{S1}[j]^2+\mathrm{S2}[j]-\mathrm{s2}[j]\right)}{(j-1)\,j\,(j+1)}\right);$$

$$\gamma\,\mathrm{sgg}[j\_]:=\mathrm{cF}*\mathrm{Tf}\left(8+\frac{16\left(-4-4\,j-5\,j^2-10\,j^3+j^4+4\,j^5+2\,j^6\right)}{(j-1)\,j^3\,(j+1)^3\,(j+2)}\right)+$$

$$\mathrm{cA}*\mathrm{Tf}\left(\frac{32}{3}+\frac{16\left(12+56\,j+94\,j^2+76\,j^3+38\,j^4\right)}{9\,(j-1)\,j^2\,(j+1)^2\,(j+2)}-\frac{160\,\mathrm{S1}[j]}{9}\right)+$$

$$\mathrm{cA}^2\left(-\left(4\left(576+1488\,j+560\,j^2-1632\,j^3-2344\,j^4+1567\,j^5\right)\right)\Big/\left(9\,(j-1)^2\,j^3\,(j+1)^3\,(j+2)^3\right)+\frac{\left(6098\,j^3+6040\,j^4+2742\,j^5\,457\,j^6\right)}{9\,(j-1)^2\,(j+1)^3\,(j+2)^3}-\frac{64}{3}+\frac{536}{9}\,\mathrm{S1}[j]+\frac{64\left(-2-2\,j-7\,j^2+8\,j^3+5\,j^4+2\,j^5\right)\mathrm{S1}[j]}{(j-1)^2\,(j+1)^2\,(j+2)^2}+\frac{32\left(1+j+j^2\right)\mathrm{s2}[j]}{(j-1)\,j\,(j+1)\,(j+2)}-16\,\mathrm{S1}[j]*\mathrm{s2}[j]+32\,\mathrm{ss}[j]-4\,\mathrm{s3}[j]\right);$$

$$\mathrm{PQQ}[j\_,Q\_]:=-\frac{\gamma\,\mathrm{sqq}[j]}{8}+\mathrm{cF}^2\left(-4\,\mathrm{S1}[j]+3+\frac{2}{j\,(j+1)}\right)\left(2\,\mathrm{S2}[j]-\frac{\mathrm{Pi}^2}{3}-\frac{2\,j+1}{j^2\,(j+1)^2}\right)+\mathrm{cF}*\mathrm{Tf}\left(-\frac{80}{9}\,\frac{1}{j-1}+\frac{8}{j^3}+\frac{12}{j^2}-\frac{12}{j}+\frac{8}{(j+1)^3}+\frac{28}{(j+1)^2}-\frac{4}{j+1}+\frac{32}{3}\,\frac{1}{(j+2)^2}+\frac{224}{9}\,\frac{1}{j+2}\right);$$

$$\mathrm{PQG}[j\_,Q\_]:=\frac{1}{2\,\mathrm{flav}[Q]}\left(\mathrm{Tf}^2\,\frac{8}{3}\left(\mathrm{S1}[j+1]\,\frac{j^2+j+2}{j\,(j+1)\,(j+2)}+\frac{1}{j^2}-\frac{5}{3}\,\frac{1}{j}-\frac{1}{j\,(j+1)}-\frac{2}{(j+1)^2}+\frac{4}{3}\,\frac{1}{j+1}+\frac{4}{(j+2)^2}-\frac{4}{3}\,\frac{1}{j+2}\right)+\mathrm{cF}*\mathrm{Tf}\left(\left(-2\,\mathrm{S1}[j+1]^2+2\,\mathrm{S1}[j+1]+10\,\mathrm{S2}[j+1]\right)\frac{j^2+j+2}{j\,(j+1)\,(j+2)}+4\,\mathrm{S1}[j+1]\left(-\frac{1}{j^2}+\frac{1}{j}+\frac{1}{j\,(j+1)}+\frac{2}{(j+1)^2}-\frac{4}{(j+2)^2}\right)-\frac{2}{j^3}+\frac{5}{j^2}-\frac{12}{j}+\frac{4}{j^2\,(j+1)}-\frac{12}{j\,(j+1)^2}-\frac{6}{j\,(j+2)}+\frac{4}{(j+1)^3}-\frac{4}{(j+1)^2}+\frac{23}{j+1}-\frac{20}{j+2}\right)+\mathrm{cA}*\mathrm{Tf}\left(\left(2\,\mathrm{S1}[j+1]^2-\frac{10}{3}\,\mathrm{S1}[j+1]-6\,\mathrm{S2}[j+1]+\mathrm{G}[j+1]-\mathrm{Pi}^2\right)\frac{j^2+j+2}{j\,(j+1)\,(j+2)}-4\,\mathrm{S1}[j+1]\left(-\frac{2}{j^2}+\frac{1}{j}+\frac{1}{j\,(j+1)}+\frac{4}{(j+1)^2}-\frac{6}{(j+2)^2}\right)-\frac{40}{9}\,\frac{1}{j-1}+\frac{4}{j^3}+\frac{8}{3}\,\frac{1}{j^2}+\frac{26}{9}\,\frac{1}{j}-\frac{8}{j^2\,(j+1)^2}+\frac{22}{3}\,\frac{1}{j\,(j+1)}+\frac{16}{(j+1)^3}+\frac{68}{3}\,\frac{1}{(j+1)^2}-\frac{190}{9}\,\frac{1}{j+1}+\frac{8}{(j+1)^2\,(j+2)}-\frac{4}{(j+2)^2}+\frac{356}{9}\,\frac{1}{j+2}\right)\right);$$

$$\mathrm{PGQ}[j\_,Q\_]:=2\,\mathrm{flav}[Q]\left(\mathrm{cF}^2\left(\left(\mathrm{S1}[j]^2-3\,\mathrm{S2}[j]-\frac{2\,\mathrm{Pi}^2}{3}\right)\frac{j^2+j+2}{(j-1)\,j\,(j+1)}+2\,\mathrm{S1}[j]\left(\frac{4}{(j-1)^2}-\frac{2}{(j-1)\,j}-\frac{4}{j^2}+\frac{3}{(j+1)^2}-\frac{1}{j+1}\right)-\frac{8}{(j-1)^2\,j}+\right.\right.$$

$$\frac{8}{(j-1)\,j^2}+\frac{2}{j^3}+\frac{8}{j^2}-\frac{1}{2\,j}+\frac{1}{(j+1)^3}-\frac{5}{2}\,\frac{1}{(j+1)^2}+\frac{9}{2}\,\frac{1}{j+1}\Bigg)+$$

$$\text{cF}*\text{cA}\,\Bigg(\Bigg(-\text{S1}[j]+5\,\text{S2}[j]-\text{G}[j]+\frac{\text{Pi}^2}{6}\Bigg)\,\frac{j^2+j+2}{(j-1)\,j\,(j+1)}+$$

$$2\,\text{S1}[j]\,\Bigg(-\frac{2}{(j-1)^2}+\frac{2}{(j-1)\,j}+\frac{2}{j^2}-\frac{2}{(j+1)^2}+\frac{1}{j+1}\Bigg)-$$

$$\frac{8}{(j-1)^3}+\frac{6}{(j+1)^2}+\frac{17}{9}\,\frac{1}{j-1}+\frac{4}{(j-1)^2\,j}-\frac{12}{(j-1)\,j^2}-\frac{8}{j^2}+\frac{5}{j}-$$

$$\frac{2}{j^2\,(j+1)}-\frac{2}{(j+1)^3}-\frac{7}{(j+1)^2}-\frac{1}{j+1}-\frac{8}{3}\,\frac{1}{(j+2)^2}-\frac{44}{9}\,\frac{1}{j+2}\Bigg)\Bigg);$$

$$\text{PGG}[j\_,\ Q\_]:=-\frac{\gamma\,\text{sgg}[j]}{8}+\text{cF}*\text{Tf}\,\Bigg(-\frac{16}{3}\,\frac{1}{(j-1)^2}+\frac{80}{9}\,\frac{1}{j-1}+\frac{8}{j^3}-\frac{16}{j^2}+\frac{12}{j}+$$

$$\frac{8}{(j+1)^3}-\frac{24}{(j+1)^2}+\frac{4}{j+1}-\frac{16}{3}\,\frac{1}{(j+1)^2}-\frac{224}{9}\,\frac{1}{j+2}\Bigg)+$$

$$\text{cA}*\text{Tf}\,\Bigg(-\frac{8}{3}\Bigg)\,\Bigg(\text{S2}[j]-\frac{1}{(j-1)^2}+\frac{1}{j^2}-\frac{1}{(j+1)^2}+\frac{1}{(j+2)^2}-\frac{\text{Pi}^2}{6}\Bigg)+$$

$$\text{cA}^2\,\Bigg(-8\,\text{S1}[j]\,\text{S2}[j]+8\,\text{S1}[j]\,\Bigg(\frac{1}{(j-1)^2}-\frac{1}{j^2}+\frac{1}{(j+1)^2}-\frac{1}{(j+2)^2}+\frac{\text{Pi}^2}{6}\Bigg)+\Bigg(8\,\text{S2}[j]-\frac{4\,\text{Pi}^2}{3}\Bigg)$$

$$\Bigg(\frac{1}{j-1}-\frac{1}{j}+\frac{1}{j+1}-\frac{1}{j+2}+\frac{11}{12}\Bigg)-\frac{8}{(j-1)^3}+\frac{22}{3}\,\frac{1}{(j-1)^2}-\frac{8}{(j-1)^2\,j}-\frac{8}{(j-1)\,j^2}-\frac{8}{j^3}-$$

$$\frac{14}{3}\,\frac{1}{j^2}-\frac{8}{(j+1)^3}+\frac{14}{3}\,\frac{1}{(j+1)^2}-\frac{8}{(j+1)^2\,(j+2)}-\frac{8}{(j+1)\,(j+2)^2}-\frac{8}{(j+2)^3}-\frac{22}{3}\,\frac{1}{(j+2)^2}\Bigg);$$

```
(*Mellin Transforms*)
md[j_, n_, αα _, β _, γ _, δ _] := Integrate[z^(j-1) * d[z, n, αα, β, γ, δ], {z, 0, 1}];

(*assumtptions:
 j+αα > 0 only valid with cutoff at j>αα_min
   β>0 valid
   δ>0 valid
    therefore β+δ>0
   therefore assumtion for Md is valid under cutoff
*)

(*functional form in mellin space*)
Md[j_, n_, αα _, β _, γ _, δ _] := (n Gamma[j + αα]
      (γ Gamma[1 + j + αα + β] Gamma[1 + β + δ] + Gamma[1 + β] Gamma[1 + j + αα + β + δ])) /
   ((Beta[2 + αα, 1 + β] + γ Beta[2 + αα, 1 + β + δ]) Gamma[1 + j + αα + β] Gamma[1 + j + αα + β + δ]);
```

```
(*Step 2: DGLAP EVOLUTION*)

(* dDj^H/dlnQ^2 = Pij*Di^H
  => Dj^H = ∫_1^BELLE/OPAL (Pij*Di^H) dlnQ

        substitute u for (ln Q)^2 → du/dQ =1/2Q → 1/2Q dQ *)

partonsLO = {Pqq, Pqg, Pgq, Pgg};
partonsNLO = {PQQ, PQG, PGQ, PGG};
NLO = False;

mP[j_, Q_, parton_] :=
  α[Q]/(2 Pi) partonsLO[[parton]][j] + If[NLO == True, (α[Q]/(2 Pi))^2 partonsNLO[[parton]][j], 0];
mff[j_, Q_, n_, αα_, β_, γ_, δ_] := Sum[mP[j, Q, p] * Md[j, n, αα, β, γ, δ], {p, 1, 4}];
mFF[j_, Q_, n_, αα_, β_, γ_, δ_] :=
 Integrate[If[qq < 1, 0, 1/(2 * qq) * mff[j, qq, n, αα, β, γ, δ]], {qq, 1, Q}]

mFF[j, OPAL, n, αα, β, γ, δ]

(*Observation: under j=0.6 mFF becomes negative
  solutions: restrictions for coefficients*)

(*Step 3: convolution with coefficient functions*)
(*definitions*)
(*Sin[θW]^2=weinberg*)
weinberg = 0.23;
coswein = 1 - weinberg;
Mz = 91.1876 (*GeV*);
(*u,c,t:*)
eu = 2/3;
Au = 1/2;
vu = 1/2 - 4/3 weinberg;
(*d,s,b:*)
ed = -1/3;
Ad = -1/2;
vd = -1/2 + 2/3 weinberg;
(*e,μ,τ:*)
ee = -1;
```

```
Ae = -1/2;
ve = -1/2 + 2 weinberg;
(*1=up, 2=down, 3=charm, 4=strange, 5=bottom, 6 would be top but is not considered*)
quarkcharges = {2/3, -2/3, -1/3, 1/3, 2/3, -2/3, -1/3, 1/3, -1/3, 1/3, 0};

(*c=3 for q, and 1 for e*)
(*Γz=332c (|Vf|^2+|Af|^2) (*MeV*)*)
Γ1= 0.332 * 3 (Abs[vu]^2 + Abs[Au]^2);
Γ2= 0.332 * 3 (Abs[vd]^2 + Abs[Ad]^2);
(*Γe=0.332(Abs[ve]^2+Abs[Ae]^2);*)
(*eq=eu;
vq=vu;*)
(*χ1a[Q_]:=*)χ1a= Compile[{Q}, 1/(16 weinberg * coswein) (Q (Q - Mz^2))/((Q - Mz^2)^2 + Γ1^2 Mz^2)];

(*χ1b[Q_]:=*)χ1b= Compile[{Q}, 1/(16 weinberg * coswein) (Q (Q - Mz^2))/((Q - Mz^2)^2 + Γ2^2 Mz^2)];


(*χ2a[Q_]:=*)χ2a= Compile[{Q}, 1/(256 weinberg^2 coswein^2) Q^2/((Q - Mz^2)^2 + Γ1^2 Mz^2)];

(*χ2b[Q_]:=*)χ2b= Compile[{Q}, 1/(256 weinberg^2 coswein^2) Q^2/((Q - Mz^2)^2 + Γ2^2 Mz^2)];

(*ehatsqr1[Q_]:=*)
ehatsqr1 = Compile[{Q}, eu^2 - 2 eu χ1a[Q] ve * vu + χ2a[Q] (1 - ve^2) (1 - (vu)^2)];
(*ehatsqr2[Q_]:=*)
ehatsqr2 = Compile[{Q}, ed^2 - 2 ed χ1b[Q] ve * vd + χ2b[Q] (1 - ve^2) (1 - (vd)^2)];
zero[Q_] := 0;

(*1=up, 2=down, 3=charm, 4=strange, 5=bottom, 6 would be top but is not considered*)
ehat = {ehatsqr1, ehatsqr2, ehatsqr1, ehatsqr2, ehatsqr1, zero(*,ehatsqr2*)};

(*coefficient1={C1q,C1g};
   coefficientL={CLq,CLg};*
   mC[j_,parton_]:=coefficient[[parton]][j];*)

mConv1[j_, Q_, n_, αα_, β_, γ_, δ_] :=
  (C1q[j] * mFF[j, Q, n, αα, β, γ, δ]) + (C1g[j] * mFF[j, Q, n, αα, β, γ, δ]);

mConvL[j_, Q_, n_, αα_, β_, γ_, δ_] :=
  (CLq[j] * mFF[j, Q, n, αα, β, γ, δ]) + (CLg[j] * mFF[j, Q, n, αα, β, γ, δ]);

mF1H[j_, Q_, n_, αα_, β_, γ_, δ_] :=
  2 * Sum[ehat[[q]][Q] * (mFF[j, Q, n[[q]], αα[[q]], β[[q]], γ[[q]], δ[[q]]] +
        α[Q]/(2 Pi) * mConv1[j, Q, n[[q]], αα[[q]], β[[q]], γ[[q]], δ[[q]]]), {q, 1, 5}] +
   Sum[ehat[[q]][Q] * (mFF[j, Q, n[[q]], αα[[q]], β[[q]], γ[[q]], δ[[q]]] +
       α[Q]/(2 Pi) * mConv1[j, Q, n[[q]], αα[[q]], β[[q]], γ[[q]], δ[[q]]]), {q, 6, 6}];
mFLH[j_, Q_, n_, αα_, β_, γ_, δ_] := α[Q]/(2 Pi) * 2 * Sum[ehat[[q]][Q] *
      (mConvL[j, Q, n[[q]], αα[[q]], β[[q]], γ[[q]], δ[[q]]]), {q, 1, 5}] +
   Sum[ehat[[q]][Q] * (mConvL[j, Q, n[[q]], αα[[q]], β[[q]], γ[[q]], δ[[q]]]), {q, 6, 6}];
```

```
(*Observation: over j=0.5 mConvL and mConv1 become negative
  solution: restrictions to coefficients*)

(**Observation: under j=0.4 negative mF1H, mFLH becomes negative over 0.5*)

(*--------------------------------------------------------------------------------------
                                                  ----------------*)

(*Contour*)
contour = 1.3;
ϕ = 3/4 * Pi;
j = contour + x * (Exp[ⅈ * ϕ]);

(*Step 4a: Mellin Inversion with NIntegrate and calculating the cross section*)

(*Coefficient functions LO*)
gu = 2 * 10^-5;
gd = 4 * 10^-5;
gc = 9 * 10^-3;
gs = 8 * 10^-4;
gb = 3 * 10^-2;
g = {gu, gd, gc, gs, gb, 0};

<< NumericalDifferentialEquationAnalysis`

(*LO*)
FFa[z_, Q_, n_, αα_, β_, γ_, δ_] :=
  1/Pi * NIntegrate[Im[(z^-j) * mFF[j, Q, n, αα, β, γ, δ]], {x, 0, 5}];
FLOa[z_, Q_, n_, αα_, β_, γ_, δ_] :=
  Sum[g[[q]] * FFa[z, Q, n[[q]], αα[[q]], β[[q]], γ[[q]], δ[[q]]], {q, 1, 5}] +
   Sum[g[[q]] * FFa[z, Q, n[[q]], αα[[q]], β[[q]], γ[[q]], δ[[q]]], {q, 6, 6}];

(*NLO*)
SF1a[z_, Q_, n_, αα_, β_, γ_, δ_] :=
  1/Pi * NIntegrate[Im[(z^-j) * mF1H[j, Q, n, αα, β, γ, δ]], {x, 0, 5}];
SFLa[z_, Q_, n_, αα_, β_, γ_, δ_] :=
  1/Pi * NIntegrate[Im[(z^-j) * mFLH[j, Q, n, αα, β, γ, δ]], {x, 0, 5}];

(*Step 5a: calculation of cross section*)

NLO = False;
σ0[Q_] := ((4 Pi * (1/137)^2 (*α[Q]^2*)) / (Q(*Q is Q2 and s = sqrt(q)*)));

crosssec[z_, Q_, n_, αα_, β_, γ_, δ_] :=
 If[
  NLO == True,
  1/Sum[ehat[[q]][Q], {q, 1, 6}] * (2 * SF1a[z, Q, n, αα, β, γ, δ] + SFLa[z, Q, n, αα, β, γ, δ]),
  (1/Sum[ehat[[q]][Q], {q, 1, 6}] * (FLOa[z, Q, n, αα, β, γ, δ]))]

(*FIT*)
(*Data Import*)
```

```
(*import*)
SetDirectory[
  DirectoryName[ToFileName["FileName" /. NotebookInformation[EvaluationNotebook[]]]]];
directory = "/media/AA54578A54575861/uni/Phenix1/thesis/FF/";
experiments = {"pi0belle", "k0belle", "opalpi", "opalk"};
(*definitions*)
fullset = Table[0, {v, 1, Length[experiments]}];
zvalues = Table[0, {v, 1, Length[experiments]}];
yields = Table[0, {v, 1, Length[experiments]}];
data = Table[0, {v, 1, Length[experiments]}];
staterr = Table[0, {v, 1, Length[experiments]}];
syserr = Table[0, {v, 1, Length[experiments]}];
err = Table[0, {v, 1, Length[experiments]}];
toterr = Table[0, {v, 1, Length[experiments]}];

energies = {BELLE, BELLE, OPAL, OPAL};

(*datause*)
For[v = 1, v ≤ Length[experiments], v++,
 fullset[[v]] =
  Select[Import[directory <> experiments[[v]] <> ".dat"], #[[1]] ≥ 0.0054 &];
 zvalues[[v]] = Take[fullset[[v]], All, {1}];
 yields[[v]] = Take[fullset[[v]], All, {2}];
 data[[v]] = Take[fullset[[v]], All, {1, 2}];
 staterr[[v]] = Take[fullset[[v]], All, {3}];
 syserr[[v]] = Take[fullset[[v]], All, {4}];
 err[[v]] = Take[fullset[[v]], {3, 4}];
 toterr[[v]] = √(staterr[[v]]^2 + syserr[[v]]^2) ;
]

(*datasets[[1]]=list of pions from belle and opal combined
   datasets[[2]]=list of kaons from belle and opal combined*)

datasets = {Join[
     Table[Append[data[[1, i]], energies[[1]]], {i, 1, Length[data[[1]]]}],
     Table[Append[data[[3, i]], energies[[3]]], {i, 1, Length[data[[3]]]}]
    ],
    Join[
     Table[Append[data[[2, i]], energies[[2]]], {i, 1, Length[data[[2]]]}],
     Table[Append[data[[4, i]], energies[[4]]], {i, 1, Length[data[[4]]]}]
    ]
   };

datasetserr = {Join[
     √(staterr[[1]]^2 + syserr[[1]]^2) , √(staterr[[3]]^2 + syserr[[3]]^2)
    ],
    Join[
     √(staterr[[2]]^2 + syserr[[2]]^2) , √(staterr[[4]]^2 + syserr[[4]]^2)
    ]
   };

(*chi² for 5 paramters, v=1: pion■ @ BELLE,
v=2: kaon■ @ BELLE, v=3: pion■ @ OPAL, v=4: kaon■ @ OPAL*)

chisquared[v_, n_, αα_, β_, γ_, δ_] := {{n[[v]], αα[[v]], β[[v]], γ[[v]], δ[[v]]},
  Sum[(crosssec[datasets[[v, ii, 1]], datasets[[v, ii, 3]], n[[v]],
        αα[[v]], β[[v]], γ[[v]], δ[[v]]] - datasets[[v, ii, 2]])^2 /
    (datasetserr[[v, ii]])^2, {ii, 1, Length[datasets[[v]]]}]}
```

```
(*multiple parameters {pi0:u+au,d+ad,s+as,c+ac,b+ab,gluon},{k0}*)
(*LO*)

NLO = False;

marcoN = {{0.367, 0.404, 0.197, 0.256, 0.469, 0.493},
   {0.054, 0.010, 0.361, 0.214, 0.147, 0.036}};
marcoα = {{-0.228, -0.228, 0.123, -0.310, -1, 108, 1.179},
   {1.018, 1.322, 0.733, 0.239, -0.464, 5.282}};
marcoβ = {{1.20, 1.20, 2.19, 4.89, 6.45, 2.83}, {1.20, 10.00, 1.20, 4.27, 7.37, 1.20}};
marcoγ = {{5.29, 5.29, 7.80, 0.00, 0.00, -1.00}, {15.00, 10.00, 20.00, 0.00, 0.00, 0.00}};
marcoδ = {{4.51, 4.51, 6.80, 0.00, 0.00, 6.76}, {6.04, 3.67, 5.28, 0.00, 0.00, 0.00}};

(*NLO*)

marcoNNLO = {{0.347, 0.380, 0.190, 0.271, 0.501, 0.279},
   {0.058, 0.016, 0.343, 0.196, 0.139, 0.017}};
marcoα NLO= {{-0.015, -0.015, 0.520, -0.905, -1, 305, 0.899},
   {0.705, 1.108, -0, 065, 0.102, -0.584, 5.055}};
marcoβ NLO= {{1.20, 1.20, 3.27, 3.23, 5.67, 1.57}, {1.20, 10.00, 1.20, 4.56, 7.42, 1.20}};
marcoγ NLO=
  {{11.06, 11.06, 16.26, 0.00, 0.00, 20.00}, {15.00, 10.00, 4.36, 0.00, 0.00, 0.00}};
marcoδ NLO= {{4.23, 4.23, 8.46, 0.00, 0.00, 4.91}, {6.02, 3.28, 3.73, 0.00, 0.00, 0.00}};


myN := If[NLO == False,
   Table[Random[Real, {0 * marcoN[[had, part]], 2 * marcoN[[had, part]]}],
    {had, 1, 2}, {part, 1, 6}], Table[Random[Real,
     {0 * marcoNNLO[[had, part]], 2 * marcoNNLO[[had, part]]}], {had, 1, 2}, {part, 1, 6}]
  ];
myα := If[NLO == False,
   Table[Random[Real, {2 * marcoα[[had, part]], 0 * marcoα[[had, part]]}],
    {had, 1, 2}, {part, 1, 6}],
   Table[Random[Real, {2 * marcoα NLO[[had, part]], 0 * marcoα NLO[[had, part]]}],
     {had, 1, 2}, {part, 1, 6}]
    ];
myβ := If[NLO == False,
   Table[Random[Real, {0 * marcoβ[[had, part]], 2 * marcoβ[[had, part]]}],
    {had, 1, 2}, {part, 1, 6}],
   Table[Random[Real, {0 * marcoβ NLO[[had, part]], 2 * marcoβ NLO[[had, part]]}],
     {had, 1, 2}, {part, 1, 6}]
    ];
myγ := If[NLO == False,
   Table[Random[Real, {0 * marcoγ[[had, part]], 2 * marcoγ[[had, part]]}],
    {had, 1, 2}, {part, 1, 6}],
   Table[Random[Real, {0 * marcoγ NLO[[had, part]], 2 * marcoγ NLO[[had, part]]}],
     {had, 1, 2}, {part, 1, 6}]
    ];
myδ := If[NLO == False,
   Table[Random[Real, {0 * marcoδ[[had, part]], 2 * marcoδ[[had, part]]}],
    {had, 1, 2}, {part, 1, 6}],
   Table[Random[Real, {0 * marcoδ NLO[[had, part]], 2 * marcoδ NLO[[had, part]]}],
     {had, 1, 2}, {part, 1, 6}]
    ];

SeedRandom[1]
results = {};
While[True,
 temp = chisquared[1, myN, myα, myβ, myγ, myδ];
 Print[temp];
 results = Append[results, temp]
   ]

results

(*Plots*)

(*for BELLE*)
```

```
pizeroN = {0.10256533196328209`, 0.31449653668345856`, 0.08021694451674993`,
   0.47608135707526783`, 0.30808441693358174`, 0.7995306325041155`};
pizeroα = {-0.1446025616990666`, -0.010231707381688817`, 0.10127099197555803`,
   -0.134444832154126`, -0.940629024017185`, 26.766149147723006`};
pizeroβ = {0.5558547991519033`, 2.1788370042309473`, 3.039122880538067`,
   5.923005663543649`, 11.650737692090516`, 0.5488261865263675`};
pizeroγ = {10.122846856196453`, 3.0229525166725764`,
   11.479583755022292`, 0.`, 0.`, -0.3236118861744443`};
pizeroδ = {7.9694332833342525`, 8.631058074244129`,
   12.409925461694824`, 0.`, 0.`, 11.626041271646699`};

zz = data[[1, All, 1]];

listcrosssec = crosssec[zz, BELLE, pizeroN, pizeroα, pizeroβ, pizeroγ, pizeroδ]

fitvals = {{zz[[1]], listcrosssec[[1]]},
   {zz[[2]], listcrosssec[[2]]}, {zz[[3]], listcrosssec[[3]]},
   {zz[[4]], listcrosssec[[4]]}, {zz[[5]], listcrosssec[[5]]},
   {zz[[6]], listcrosssec[[6]]}, {zz[[7]], listcrosssec[[7]]},
   {zz[[8]], listcrosssec[[8]]}, {zz[[9]], listcrosssec[[9]]},
   {zz[[10]], listcrosssec[[10]]}, {zz[[11]], listcrosssec[[11]]},
   {zz[[12]], listcrosssec[[12]]}, {zz[[13]], listcrosssec[[13]]},
   {zz[[14]], listcrosssec[[14]]}, {zz[[15]], listcrosssec[[15]]},
   {zz[[16]], listcrosssec[[16]]}, {zz[[17]], listcrosssec[[17]]},
   {zz[[18]], listcrosssec[[18]]}, {zz[[19]], listcrosssec[[19]]},
   {zz[[20]], listcrosssec[[20]]}, {zz[[21]], listcrosssec[[21]]},
   {zz[[22]], listcrosssec[[22]]}, {zz[[23]], listcrosssec[[23]]},
   {zz[[24]], listcrosssec[[24]]}, {zz[[25]], listcrosssec[[25]]},
   {zz[[26]], listcrosssec[[26]]}, {zz[[27]], listcrosssec[[27]]},
   {zz[[28]], listcrosssec[[28]]}, {zz[[29]], listcrosssec[[29]]},
   {zz[[30]], listcrosssec[[30]]}, {zz[[31]], listcrosssec[[31]]},
   {zz[[32]], listcrosssec[[32]]}, {zz[[33]], listcrosssec[[33]]},
   {zz[[34]], listcrosssec[[34]]}, {zz[[35]], listcrosssec[[35]]},
   {zz[[36]], listcrosssec[[36]]}, {zz[[37]], listcrosssec[[37]]},
   {zz[[38]], listcrosssec[[38]]}, {zz[[39]], listcrosssec[[39]]},
   {zz[[40]], listcrosssec[[40]]}, {zz[[41]], listcrosssec[[41]]},
   {zz[[42]], listcrosssec[[42]]}, {zz[[43]], listcrosssec[[43]]},
   {zz[[44]], listcrosssec[[44]]}, {zz[[45]], listcrosssec[[45]]},
   {zz[[46]], listcrosssec[[46]]}, {zz[[47]], listcrosssec[[47]]},
   {zz[[48]], listcrosssec[[48]]}, {zz[[49]], listcrosssec[[49]]},
   {zz[[50]], listcrosssec[[50]]}, {zz[[51]], listcrosssec[[51]]},
   {zz[[52]], listcrosssec[[52]]}, {zz[[53]], listcrosssec[[53]]},
   {zz[[54]], listcrosssec[[54]]}, {zz[[55]], listcrosssec[[55]]}};

ListLogPlot[data[[3]]]
```

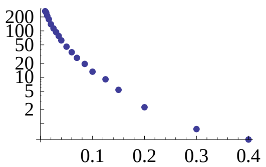


```
ListLogPlot[{fitvals}, Joined → True]
```

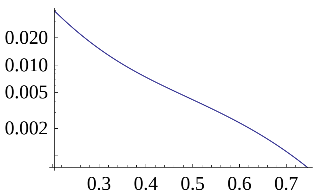

```
Show[ListLogPlot[data[[1]]],
 ListLogPlot[{fitvals}, Joined → True], AxesLabel → {z, (1/σtot) (dσ^h/dz)}]
```

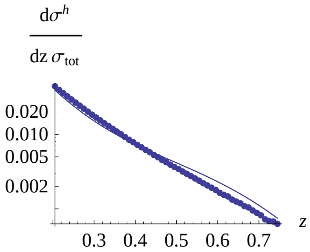

Abstract / Zusammenfassung

Um den Prozess der Hadronproduktion zu erklären sind sowohl theoretische Vorhersagen, also auch experimentelle Ergebnisse nötig. Störungstheoretisch berechnete Wirkungsquerschnitte, gemeinsam mit zwei nicht rein theoretisch berechenbaren Komponenten, dienen zur Beschreibung von Streuvorgängen, in denen Hadronen beobachtet werden können. Erstere können ohne zusätzliche Information im Rahmen der Quantenchromodynamik, der Eichtheorie der starken Wechselwirkung, berechnet werden, die letzteren zwei Komponenten hingegen, benötigen zur Bestimmung zusätzliche Informationen, die nur aus Experimentellen Daten gewonnen werden können. Diese beiden Teile der Beschreibung von Hadronisationsprozessen sind Parton- Verteilungsfunktionen (PDFs) und Framentationsfunktionen (FFs), wobei PDFs eine Wahschreinlichkeitsverteilung angeben, ein Parton innerhalb eines Hadrons zu finden, mit einem gewissen Impulsanteil des "Mutter"-Hadrons. FFs hingegen, auf deren Berechnung sich diese Arbeit beschränkt, beschreiben eine Wahrscheinlichkeitsverteilung ein Hadron zu finden mit einem gewissen Impulsanteil des erzeugenden Partons. Fragmentationsfunktionen beschreiben somit einen Einteilchen-Endzustand eines Streuprozesses wohingegen Parton-Verteilungsfunktionen Aussagen über ein Anfangsteilchen machen.
Aufgrund einer, für nicht-abelsche Eichtheorien spezifischen Eigenschaft, der Asymptotischen Freiheit, sind störungstheoretische Berechnungen solcher physikalischer Vorgänge nur für relativ hohe Energien möglich. Der eigentliche Hadronisationsprozess findet allerdings bei niedrigeren Energien statt und seine vollständige Beschreibung benötigt daher die zusätzliche Verwendung von experimentellen Ergebnissen.
Die so erhaltenen Funktionen erlauben Aussagen über Details von Reaktionen, die in dieser Genauikeit von keinem theoretischen Modell allein erreicht werden können und sind daher für die Beschreibung von Nucleon-Strukturen von äußerst hohem Wert.
Ein großer Vorteil der Berechnung von Fragmentationsfunktionen liegt in ihrer Prozessunabhägigkeit. Da die Eigenschaften eines Hadrons die gleichen sind, unabhängig von der Art seiner Produktion, ist eine solche Funktion nicht nur für gleiche Experimente anderer Energien anwendbar, sondern kann auch Aussagen über völlig andere phyikalische Prozesse treffen, in denen Hadronen erzeugt werden. Diese Tatsache macht Fragmentationsfunktionen für eine Vielzahl von Anwendungen in der Hochenergiephysik zu einem wertvollen Instrument.
In dieser Arbeit wurden FFs berechnet indem zuerst der störungstheoretisch bestimmbare Teil ermittelt wurde und schließlich der gesamte Wirkungsquerschnitt mit Hilfe einer Chi^2-Minimierung, zu Daten aus Elektron- Positron-

Annihilationsexperimenten berechnet. Die vollständige Beschreibung des Wirkungsquerschnittes beinhaltet eine Lösung der Renormierungsgruppengleichung, um die quantenchromodynamische Kopplunsstärke $\alpha_S(Q^2)$, in Abhängigkeit der Energie Q^2 zu bestimmen, sowie die Evolution mit Q^2, die den Vergleich von Ergebnissen bei verschiedenen Energien ermöglicht. Dafür ist es notwending eine Anfangsparametisierung D_i^H, der sogenannten DGLAP-Evolution zu unterziehen. Diese von Dokshitzer, Gribov, Lipatov, Altarelli und Parisi entwickelte Evolutionsgleichung enthält Faltungen der Parametrisierung mit "Splittingfunctions", welche die Wahrscheinlichkeit angeben, dass ein Parton ein weiteres Parton (beispielsweise ein Quark oder Gluon), mit einem bestimmten Impulsanteil des ursprünglichen abstrahlt. Um den gesamten Wirkungsquerschnitt $\frac{1}{\sigma_{tot}}\frac{d\sigma^H}{dz}$ bestimmen zu können muss schließlich die Wahschreinlichkeit der eigentlichen Erzeugung der Partonen aus e^+e^- und deren Imulsanteil miteinbezogen werden, was durch Faltungen mit "Coefficientfunctions" erreicht wird.
Um diese, nur numerisch durchführbaren Berechnungen effizient möglich zu machen, ist es notwendig im Mellin-Raum zu arbeiten, in dem sich Faltungen zu Produkten reduzieren lassen. Nun ist es möglich die freien Parameter in D_i^H durch einen Fit an Daten zu bestimmen.
In dieser Arbeit wurden oben genannte Berechnungen durchgeführt, Fragmentationsfunktionen in Leading Order bestimmt und mit Daten aus den e^+e^--Annihilationsexperimenten OPAL und BELLE verglichen. Eine Erweiterung um die Berechnung in Next-to-Leading Order gäbe zusätzliche Informationen, sowie besser konvergierende Fits und war aufgrund des angewendeten Fit-Programmes in dieser Analyse nicht möglich.

Bibliography

[1] R.K. Ellis, W.J. Stirling, and B.R. Webber. *QCD and Collider Physics.* Cambridge University Press, 1996.

[2] Schramm Greiner and Stein. *Quantum Chromodynamics 2nd Edition.* Springer, 2002.

[3] M. Glück, E. Reya, M. Stratmann, and W. Vogelsang. Models for the polarized parton distributions of the nucleon. *Phys. Rev. D*, 63 094005, 2001.

[4] R. G. Roberts R.S. Thorne, A. D. Martin and W. J. Stirling. Recent progress in parton distributions and implications for lhc physics. *arXiv:hep-ph/0507015v1*, 2005.

[5] R. Sassot D. de Florian and M. Stratmann. Global analysis of fragmentation functions for pions and kaons and their uncertainties. *Phys. Rev. D*, 75 094009, 2007.

[6] S. Kretzer. Fragmentation functions from flavour-inclusive and flavour-tagged e^+e^- annihilations. *arXiv:hep-ph0003177v2*, 2000.

[7] O. Biebel, P. Nason, and B.R. Webber. Jet fragmentation in e^+e^- annihilation. *arXiv:hep-ph0109282*, 2001.

[8] M. Hirai, S. Kumano, T.-H. Nagai, and K. Sudoh. Determination of fragmentation functions and their uncertainties. *Phys. Rev. D*, 75 114010, 2007.

[9] R.L. Jaffe. Spin, twist and hadron structure in deep inelastic processes. *arXiv:hep-ph/9602236v1*, 1995.

[10] M. Leitgab. *Master's Thesis: Precision Measurement of Pion and Kaon Multiplicities in e^+e^- Annihilation at $\sqrt{s} = 10.52$ GeV.* July 2008.

[11] M. Stratmann D. de Florian and R. Sassot. Fragmentation functions for pions, kaons, protons and charged hadrons. *arXiv:0708.0769v1 [hep-ph]*, 2007.

[12] G. Kramer S. Albino, B.A. Kniehl. Fragmentation functions for light charged hadrons with complete quark flavour separation. *Nuclear Physics B*, 725:181–206, 2005.

[13] B.A. Kniehl, G. Kramer, and B. Pötter. Fragmentation functions for pions, kaons and protons at next-to-leading order. *arXiv:hep-ph/0010289v1*, 2000.

[14] B.A. Kniehl, G. Kramer, and B. Pötter. Testing the universality of fragmentation functions. *arXiv:hep-ph/0011155v1*, 2000.

[15] Et at. J. Abdallah. Study of leading hadrons in gluon and quark fragmentation. *Physics Letters, Section B: Nuclear, Elementary Particle and High-Energy Physics*, 643:147–157, 2006.

[16] Et al. K. Abe. Design and performance of the sld vertex detector: A 307 mpixel tracking system. *Nuclear Instruments and Methods in Physics Research, Section A: Accelerators, Spectrometers, Detectors and Associated Equipment*, 400, 1997.

[17] Et at. D. Decamp. Aleph: A detector for electron-positron annihilations at lep. *Nuclear Inst. and Methods in Physics Research, A*, 294: 121–178, 1990.

[18] M. Hirai, S. Kumano, T.-H. Nagai, and K. Sudoh. Determination of fragmentation functions and their uncertainties from $e^+ + e^- \to h + x$ data. *arXiv:hep-ph/0612009v1*, 2007.

[19] M. Hirai, S. Kumano, T.-H. Nagai, and K. Sudoh. Global analysis for determining fragmentation functions and their uncertainties in light hadrons. *arXiv:0705.2791v1 [hep-ph]*, 2007.

[20] Et al C. Amsler. The review of particle physics. *Physics Letters B*, 667.

[21] M. Stratmann D. de Florian and W. Vogelsang. Qcd analysis of unpolarized and polarized λ-baryon production in leading and next-to-leading order. *arXiv.org:hep-ph/9711387v1*, 1997.

[22] G. Altarelli and G. Parisi. Asymptotic freedom in parton language. *Nuclear Physics B*, 126:298–318, 1977.

[23] Yu.L. Dokshitzer. Calculation of the structure functions for deep inelastic scattering and $e + e-$ annihilation by perturbation theory in quantum chromodynamics. *Sov.Phys. JETP*, 46:641, 1977.

[24] L.N. Lipatov V.N. Gribov. Deep inelastic e-p scattering in perturbation theory. *Sov.J.Nucl.Phys.*, 15:438, 1972.

[25] B. Mele and P. Nason. The fragmentation function for heavy quarks in qcd. *Nuclear Physics B*, 361:626–644.

[26] E.G. Floratos and C. Kounnas. Higher order qcd effects in inclusive annihilation and deep inelastic scattering. *Nuclear Physics B*, 192: 417–462.

[27] G. Curci and W. Furmanski. Evolution of parton densities beyone leading order, the non-singlet case. *Nuclear Physics B*, 175:27–92.

[28] A. Piccione. Solving the altarelli–parisi equations with truncated moments. *Physics Letters B*, 518:207–213, 2001.

[29] David A. Kosower. Evolution of parton distributions. *arXiv:hep-ph/9706213v2*, 1997.

[30] M. Shah. *A Note on Mellin Inversion Formula.* 1971.

[31] M. Glück, E. Reya, and A. Vogt. Dynamical parton distributions revisited. *Eur.Phys.J. C, arXiv:hep-ph9806404v1*, 5, 1998.

[32] M. Glück and E. Reya. Operator mixing and scaling deviations in asymptotically free field theories. *Phys. Rev. D*, 14.

[33] B.A. Kniehl, G.Kramer, and B.Pötter. Strong coupling constant from scaling violations in fragmentation functions. *arXiv:hep-ph/0003297v1*, 2000.

[34] Et al. The OPAL Collaboration, G. Abbiendi. Multiplicities of π^0, η, k^0 and of charged particles in quark and gluon jets. *arXiv:hep-ph/9706213v2*, 1997.

[35] The OPAL Collaboration. The opal detector. *http://opal.web.cern.ch/Opal/tour/detector.html*, 1989-2000.

[36] M. Glück, E. Reya, and A. Vogt. Parton fragmentation into photons beyond leading order. *Phys. Rev. D*, 48.

[37] S. Narison. *QCD as a Theory of Hadrons, From Partons to Confinement*. Cambridge University Press, 2004.

[38] H. David Politzer. *Asymptotic Freedom: An Approach to Strong Interactions*. 1974).

Curriculum Vitae

Person

Name:	Patricia Maria Francisconi
Date of birth:	1985-03-08
Place of birth:	Schladming, Styria
Citizenship:	Austria
email:	patrciafrancisconi@gmail.com

Education

2009-12	Master's Thesis submitted: "QCD Analysis of Hadron Multiplicities and Determination of Fragmentation Functions in e^+e^--annihilation from BELLE and LEP data" supervised by Prof. W. Grimus at the University of Vienna and Prof. M. Grosse-Perdekamp at the University of Illinois at Urbana-Champaign
2007-08 until 2008-12	Research for Masters Thesis at the University of Illinois at Urbana-Champaign
2006-08 until 2006-12	Exchange Semester at the University of Illinois at Urbana-Champaign
2005-03-01	Enrollment in Master's Program in Physics at the University of Vienna
2003-10-01	Enrollment in Master's Program in Astronomy and Biology at the University of Vienna
2003-06	Graduated High School at the "Bundesrealgymnasium Waidhofen/Ybbs" with Honors
1995-09 until 1999-06	Junior High School at the "Bundesrealgymnasium Waidhofen/Ybbs" with average Grades of less than 1.5 in all four years
1991-09 1995-06	Elementary school at the "Volksschule Zell/Ybbs" with average Grades of less than 1.5 in all four years

Professional Experience

2007-08 until 2008-12	Research Assistant at the Nuclear Physics Lab at the University of Illinois at Urbana-Champaign
2004 until 2006	Libaray Assistant at the Central Physics Library in Vienna
2005-07 until 2005-10	Diveguide and Course Assistant at Koh Tao Cottage Diving Resort in Koh Tao, Thailand
2004-08 until 2004-10	Mail Delivery (2 months, during summer vacation)
2004	Waitress (6 months, besides studying)
2003-07	Secretary (2 months, during summer vacation)

Scientific Experiences

2007-08 until 2008-12	Research Assistant at the Nuclear Physics Lab at the University of Illinois at Urbana-Champaign

Additional Skills and Experiences

- Advanced Computer Knowledge in Windows and Linux
- Working with Mathematica at an Advanced Level
- European Computer Driving License
- Top ten ranking in the Austrian Association of Astronomy with High School Graduation work on "Neutrinos and their Significance in Astrophysics"
- PADI and CMAS certified Diveguide and Course Assistant
- Fluent in English
- Cambridge Certificate of Advanced English
- TOEFL Certificate in English
- Advanced knowledge of French
- Diplome European de la Langue Francais (European French Language Diploma)
- Advanced knowledge of Spanish
- Student Representative for 6 years
- Forest work in a forest of about 7 ha.

Theses

Francisconi, P. M.: "QCD Analysis of Hadron Multiplicities and Determination of Fragmentation Functions in e^+e^--annihilation from BELLE and LEP data", Diplomarbeit (2009)

Francisconi, P. M.: "Neutrinos und deren Bedeutung in der Astrophysik", Fachbereichsarbeit aus Physik (2003)

Other Activites

Voice and Theater Education since 1999

Diveguide since 2005